# Catalytic Acid−Base Groups in Yeast Pyruvate Decarboxylase. 3. A Steady-State Kinetic Model Consistent with the Behavior of both Wild-Type and Variant Enzymes at All Relevant pH Values†

Eduard A. Sergienko* and Frank Jordan*

*Department of Chemistry and Program in Cellular and Molecular Biodynamics, Rutgers, The State University of New Jersey, Newark, New Jersey 07102*

*Received December 18, 2000; Revised Manuscript Received April 17, 2001*

ABSTRACT: The widely quoted kinetic model for the mechanism of yeast pyruvate decarboxylase (YPDC, EC 4.1.1.1), an enzyme subject to substrate activation, is based on data for the wild-type enzyme under optimal experimental conditions. The major feature of the model is the obligatory binding of substrate in the regulatory site prior to substrate binding at the catalytic site. The activated monomer would complete the cycle by irreversible decarboxylation of the substrate and product (acetaldehyde) release. Our recent kinetic studies of YPDC variants substituted at positions D28 and E477 at the active center necessitate some modification of the mechanism. It was found that enzyme without substrate activation apparently is still catalytically competent. Further, substrate-dependent inhibition of D28-substituted variants leads to an enzyme form with nonzero activity at full saturation, requiring a second major branch point in the mechanism. Kinetic data for the E477Q variant suggest that three consecutive substrate binding steps may be needed to release product acetaldehyde, unlikely if YPDC monomer is the minimal catalytic unit with only two binding sites for substrate. A model to account for all kinetic observations involves a functional dimer operating through alternation of active sites. In the context of this mechanism, roles are suggested for the active center acid−base groups D28, E477, H114, and H115. The results underline once more the enormous importance that both aromatic rings of the thiamin diphosphate, rather than only the thiazolium ring, have in catalysis, a fact little appreciated prior to the availability of the 3-dimensional structure of these enzymes.

Pyruvate decarboxylase catalyzes the non-oxidative decarboxylation of pyruvate to acetaldehyde (Aa)[1] and requires thiamin diphosphate (ThDP) and Mg(II) as cofactors. Yeast pyruvate decarboxylase (YPDC, EC 4.1.1.1) is an enzyme consisting of four identical subunits (*1*, *2*). The ThDP is bound at the interface created by two subunits that form a tight dimer. Two of these dimers form a loose tetramer usually referred to as a "dimer of dimers".

Pyruvate decarboxylases from all sources, except *Zymomonas mobilis* (ZmPDC), exhibit allosteric activation by the substrate pyruvate (*3*) or the substrate analogue pyruvamide (*4*), a compound that cannot be decarboxylated. This activation is believed to entail a slow conformational change involving the entire enzyme molecule. Inhibition by the substrate (widely observed with pyruvate decarboxylases from various sources) is an additional phenomenon complicating the kinetic mechanism of YPDC that is yet poorly understood. It was suggested that perhaps the intervention of the carboligase side reactions catalyzed by YPDC was responsible for the apparent inhibition (*5*). A minimal model for the YPDC kinetic mechanism was proposed for substrate activation (see Scheme 1) which could account for the experimental data for wild-type YPDC at or near the optimum pH of 6.0 (*6*). Briefly, the principal mechanism was described in terms of a sequence of two reversible binding steps separated by a slow conformational change and followed by two irreversible catalytic reactions. One additional reversible substrate binding step was included to explain substrate inhibition; the source of the inhibition was tentatively attributed to the carboligase side reaction. The rates of the irreversible steps in Scheme 1, and as a consequence their rate-limiting effects on the entire reaction, were suggested to be equal (*5*, *6*).

The X-ray structure of YPDC has been determined both in the absence (*7*, *8*) and in the presence (*9*) of a 300 mM concentration of the substrate analogue pyruvamide, possibly resulting in nonactivated and activated forms. Each enzyme

† This work was supported by NIH Grant GM-50380, NSF Training Grant BIR 94/13198 in Cellular and Molecular Biodynamics (F.J., PI), and the Rutgers University Busch Biomedical Fund and Roche Diagnostics Corp., Indianapolis, IN. Presented in part at the ASBMB annual meeting, Boston, MA, June 2000.

* To whom correspondence should be addressed. E.A.S.: Tel 973-353-5727, FAX 973-353-1264, E-mail edouard@andromeda.rutgers.edu. F.J.: Tel 973-353-5470, FAX 973-353-1264, E-mail: frjordan@andromeda.rutgers.edu.

[1] Abbreviations: ThDP, thiamin diphosphate; Aa, acetaldehyde; Ac, acetoin; Al, acetolactate; ADC, acetolactate decarboxylase; ADH, alcohol dehydrogenase (yeast); BDH, butanediol dehydrogenase; BFD, benzoylformate decarboxylase; LDH, lactate dehydrogenase; PA, pyruvamide; WT YPDC, yeast pyruvate decarboxylase from *Saccharomyces cerevisiae* overexpressed in *E. coli*; E477Q, D28A, and D28N are variants of this enzyme with the indicated substitutions; ZmPDC, pyruvate decarboxylase isolated from *Zymomonas mobilis*; HEThDP, C2α-hydroxyethylthiamin diphosphate; LThDP, C2α-lactylthiamin diphosphate; EnThDP or enamine, C2-hydroxyethylidenethiamin diphosphate; BDThDP, 2-(2,3-dihydroxy-2-*n*-butyl)thiamin diphosphate, the C2 adduct of ThDP and acetoin.

10.1021/bi002857e CCC: $20.00 
Published on Web 05/31/2001

Scheme 1

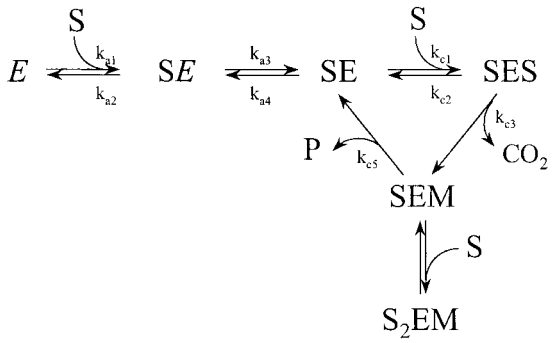


form exhibits nonequivalence of the two active sites present in the crystallographically determined dimer. The conformational change resulting from the activation of the enzyme increases this apparent nonuniformity of the active sites and gives rise to both "open" and "closed" active sites. However, to our knowledge this structural difference of the active sites has never been addressed in the functional characterization of the enzyme.

The rate expression heavily emphasizes the rates of the enzyme species that are present at the highest concentration, or have the highest catalytic rates. Therefore, the presence of some enzyme species may go unnoticed if they are present in negligible concentrations. In our recent paper on the related enzyme benzoylformate decarboxylase (BFD, ref *10*), an alternate substrate was utilized, resulting in the slow release of product and enabling us to observe features of the catalytic cycle that are not visible in the steady-state kinetic results. The ability to monitor the appearance and disappearance of enzyme-bound intermediates led to results requiring an explanation that invokes the interaction between the active sites of this tetrameric enzyme. The observation of substrate binding in the first site, thereby promoting the decarboxylation of the substrate in the second active site, led to the proposal that a pair of active sites act in an anti-concerted manner.

In the current work, instead of changing the substrate, the active site of the enzyme was changed. Most of the detailed kinetic studies of YPDC were earlier carried out on the wild-type enzyme (*5, 6*) under optimal conditions. Utilization of YPDC with an altered active site allowed us to observe previously undetected peculiarities of the YPDC mechanism. In the first paper of this series (*11*), preparation and steady-state kinetic studies were reported for the four active center variants, D28A, H114F, H115F, and E477Q, creating neutral substitutions at the four acid−base residues poised to participate in the reaction mechanism. It was concluded that while all four residues affect transition states both pre- and post-decarboxylation (i.e., at low and at saturating substrate concentrations), it is unlikely that any of the four residues is involved in the first, most crucial step, generation of the conjugate base at position C2 of the coenzyme. In the second paper (*12*), we examined the carboligase side reactions of the D28A, D28N, and E477Q variants and found that the substitutions converted the D28A and D28N variants to an acetolactate synthase and the E477Q variant to an acetoin synthase, producing these chiral compounds with high enantiomeric excess. The experiments also allowed us to determine whether pre- or post-decarboxylation events are rate-determining with the variants. Here we report our findings on the kinetic behavior of variant YPDCs with substitutions at D28 and E477, and suggest an explanation for all of the kinetic observations within the framework of a new kinetic model invoking alternating active sites. The model put forth can account for all of the kinetic observations, both with wild-type and with variant enzymes, at all pH values studied; the model is also consistent with the structural data published for YPDC so far. Finally, we propose roles for the D28 and E477 side chains on the basis of the evidence presented in the three papers in this series.

## EXPERIMENTAL PROCEDURES

The preparation of the YPDC variants and the purification and assay, along with the buffers used, the novel continuous kinetic assays developed for acetoin and acetolactate, and the instruments used in this series of studies, were presented in the previous two papers (*11, 12*).

The equations used in the studies include the original Hill equation (which did not incorporate substrate inhibition) and its variation including substrate inhibition and nonzero limiting rate. Several versions of the transformed Hill equation were suggested in the literature (*13, 14*). The two versions below could adequately describe all our data.

$$v = \frac{V_{max}[S]^{n_H}}{S_{0.5}{}^{n_H} + [S]^{n_H}(1 + [S]/K_i)} \quad (1)$$

$$v = \frac{V_{max}[S]^{n_H} + V_f[S]^{(n_H+1)}/K_i}{S_{0.5}{}^{n_H} + [S]^{n_H}(1 + [S]/K_i)} \quad (2)$$

Equation 1 (henceforth called the "simple Hill equation with inhibition" or 4-parameter Hill equation) was utilized when only insignificant substrate inhibition was observed, whereas eq 2 (the "extended Hill equation" or 5-parameter Hill equation) was sufficient to describe the data with inhibition and nonzero activity after full saturation with substrate. Equation 1 is a particular form of eq 2, in which $V_f = 0$. We realize that as any for Hill-type equation, eqs 1 and 2 are only approximations. Therefore, even if inhibition by substrate might have been allosteric in nature, no attempt was made to change the equations. One reason is that including an additional parameter (Hill coefficient for inhibition) in the power of the substrate with $V_f$ [e.g., utilizing $V_f[S]^{(n_H+k)}$] did not provide any significant improvement, since in this case the values of the two power coefficients became too interdependent, the same complication as noticed by others (*14*).

*Evaluation of Different Kinetic Models.* Two models were compared using residual plots and the *F*-statistic (*15*). In brief, the residual sum-of-squares ($RSS_1$ and $RSS_2$) for the two models (one of which is an extension of the other) were obtained through a fit with the SigmaPlot software. The quotient *Q* (defined in eq 3) was calculated as

$$Q = \frac{(RSS_1 - RSS_2)(n - p_2)}{RSS_2(p_2 - p_1)} \quad (3)$$

where $RSS_1$ and $RSS_2$ and $p_1$ and $p_2$ are the residual sum-of-squares and number of parameters in the two models and *n* is the number of data points in the experiment. The quotient

Scheme 2

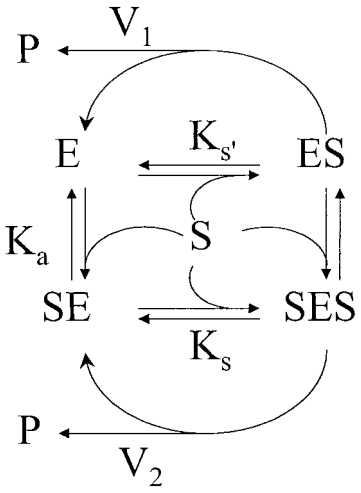


was then compared with the *F*-statistic $F(p_2 - p_1, n - p_2)$ at the desired level of probability.

*Simulation of the Kinetic Data for Testing the Earlier Kinetic Model for YPDC.* Data were simulated with the SigmaPlot software according to the equation for a two-site model with random binding in the regulatory and active sites (depicted in Scheme 2):

$$v = \frac{V_1[S]/K_{s'} + V_2[S]^2/K_aK_s}{1 + [S]/K_{s'} + [S]/K_a + [S]^2/K_aK_s} \quad (4)$$

where $K_a$ is the kinetic dissociation constant of the regulatory site, $V_1$ and $V_2$ are maximum velocities, and $K_{s'}$ and $K_s$ are kinetic dissociation constants of the active site of the nonactivated and activated enzyme form, respectively. The substrate concentration ([S]) was changed from 0.01 to 100 mM in equal increments on the logarithmic scale to give a total of 41 points. The range of dissociation constants selected (combinations in the range of 0.5−20 mM) reflects the values of the actual constants of YPDC under different conditions. Combinations that would have resulted in the observed substrate inhibition (*16*) were avoided. Values of $V_2$ were held constant and equal to 1, whereas values of $V_1$ were changed from 0 to 1. In this manner, the ratio of $V_1/V_2$ was varied from 0 to 1. The simulated data were then fitted to a Hill equation and to the equation published by the groups of Schellenberger and Hübner at Halle, and Schowen at Kansas (*5*, *6*), henceforth referred to as the SHS model.

## RESULTS

*Wild-Type YPDC.* As expected, steady-state kinetic data for the wild-type YPDC are characterized by a sigmoidal dependence on substrate concentration. While the plateau of WT YPDC catalytic activity is very broad with nearly identical values of $V_{max}$ in the pH range of 5.5−7.2, the enzyme is most efficient around pH 5.8−6.0. This pH is characterized by the maximum values of the Hill coefficient (1.58 ± 0.08) and $V_{max}/S_{0.5}$ attained, with an $S_{0.5}$ of 0.97 ± 0.037 mM. A change of pH to either side from the optimum value causes the Hill coefficient to decrease approximately 0.2 unit per unit of pH. Rather modest inhibition with high substrate concentration was also observed; its mechanism therefore could not be delineated with the WT YPDC.

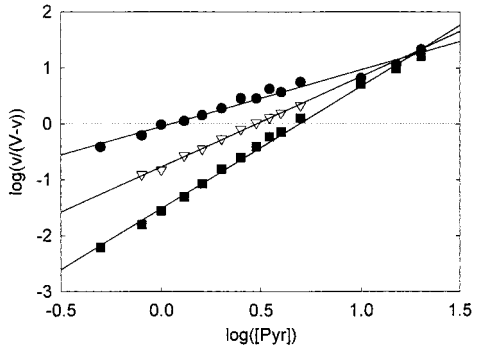


FIGURE 1: Hill plot for the pyruvate-dependent activities of the E477Q variant. Acetaldehyde formation was measured in the standard pH buffer at pH 5.1 (closed circles), pH 6.0 (open triangles), and pH 6.9 (closed squares) in the presence of 5 mM $MgCl_2$, 1 mM ThDP, 0.14 mM NADH, and 22.5 units/mL ADH. Straight lines represent the best fit of data with the slopes ($n_H$) 1.017 ± 0.046, 1.619 ± 0.0345, and 2.188 ± 0.042 for pH 5.1, 6.0, and 6.9, respectively. Half-saturation concentrations ($S_{0.5}$) are calculated from intersections of the data curves with the abscissa equal to 1.10, 2.98, and 4.89 mM, respectively.

Table 1: Kinetic Parameters for Pyruvate-Dependent Acetaldehyde Formation for the E477Q Variant at Different pH Values

| parameters | pH 5.1 | pH 6.0 | pH 6.9 |
|---|---|---|---|
| $V_{max}$ (units/mg) | 0.0233 ± 0.00044 | 0.101 ± 0.0078 | 0.120 ± 0.0012 |
| $S_{0.5}$ (mM) | 0.925 ± 0.077 | 2.900 ± 0.346 | 4.576 ± 0.136 |
| $n_H$ | 1.019 ± 0.092 | 1.673 ± 0.221 | 2.206 ± 0.128 |
| $K_i$ (mM) | (1436 ± 1387)[a] | 112.2 ± 26.4 | (1872 ± 1475)[a] |

[a] Values in parentheses were calculated in a separate fitting procedure and are shown for reference.

*Cooperativity Observed with the E477Q Variant.* The E477Q variant exhibited much more complex kinetic properties than the WT YPDC. Substrate-dependent acetaldehyde production by this variant is uniquely affected by pH. While at pH 6.0 the behavior of this variant is similar to WT YPDC, with a Hill coefficient equal to 1.5−1.6 (though with somewhat stronger substrate inhibition), at lower and higher pH major differences become apparent. Substrate inhibition disappeared both below and above pH 6.0, but the Hill coefficient increased monotonically with increasing pH (Figure 1). At pH 5.0, no cooperativity was observed, whereas at pH above 7.0 the Hill coefficient was significantly larger than 2.0, reaching a value of 2.6 [see the first paper of the series (*11*)]. Both maximal velocity and half-saturation concentration increased with increasing pH (see Table 1).

*Substrate and Product Inhibition Exhibited by the D28A and D28N Variants.* Valuable insight into the nature of substrate inhibition was obtained with the variants in which D28 was substituted; these were characterized by an extremely high degree of cooperativity and substrate inhibition. The Hill coefficient for pyruvate-dependent acetaldehyde formation for the D28N (Figure 2) and the D28A (Figure 3A) variants was equal to 2.1−2.2. Pyruvate-dependent acetoin formation by the D28A variant has a slightly lower Hill coefficient of 1.87 (see Figure 3A). Inhibition with pyruvate was characterized by an anomalously low inhibition constant $K_i$, approximately of the same order of magnitude as the half-saturation constant $S_{0.5}$ (Table 2); therefore, the substrate-dependent rate never reaches the theoretical $V_{max}$ value. Another surprising feature was that the rate of both acetaldehyde and acetoin formation at saturating concentra-

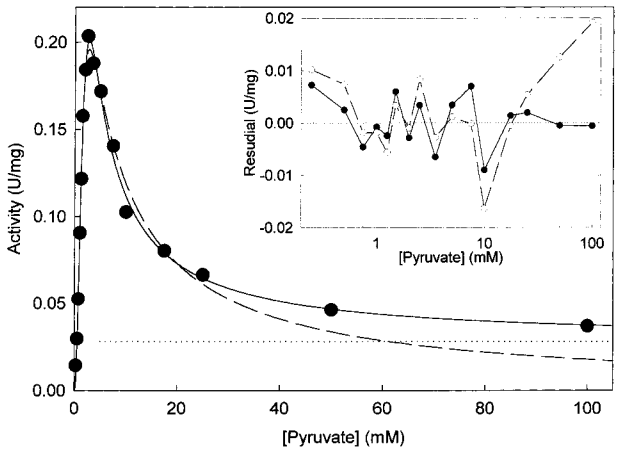


FIGURE 2: Pyruvate-dependent acetaldehyde formation by the D28N variant at pH 6.0. Conditions are the same as in Figure 1, except pH 6.0, 0.3 mM NADH, 20 units/mL ADH, and a light path of 0.45 cm were used. The reaction was started by addition of the D28N variant to a concentration of 0.07 mg/mL. The solid line represents the best fit of the data to the extended Hill equation (eq 2). The limiting rate is shown for reference as a dotted line. For comparison, the result of the fit to the simple Hill equation with inhibition (eq 1) is shown as a dashed line. The residual plot for the data fitted with eq 1 (open circles) and with eq 2 (closed circles) for both equations is shown in the inset.

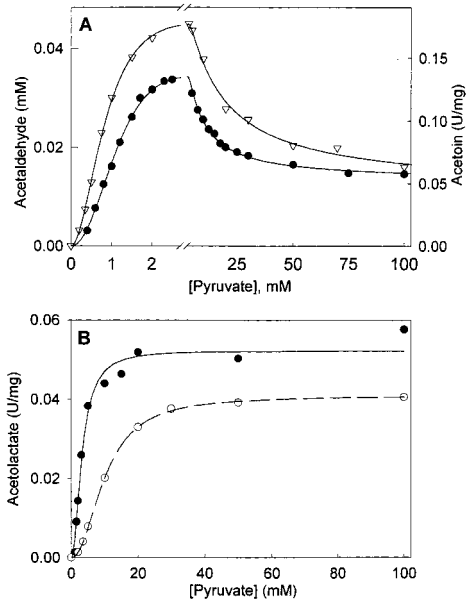


FIGURE 3: Pyruvate-dependent product formation rates of the D28A variant. All products were measured in 0.1 M MES, pH 6.0, 1 mM ThDP, 5 mM $MgCl_2$ using the relevant coupled reaction. Acetaldehyde (panel A, closed circles) and acetolactate (panel B, closed circles) were estimated in the absence of externally added acetaldehyde. Acetoin (panel A, open triangles) and acetolactate (panel B, open circles) were measured in the presence of 200 mM acetaldehyde. The *y*-scales in panel A are proportional to $v_0$.

tion of pyruvate leveled off to a constant value $V_f$, approximately an order of magnitude lower than the predicted $V_{max}$ value (Figures 2 and 3). The fitted results for D28N-assisted acetaldehyde formation (Figure 2) clearly show that $V_f$ has a nonzero value, as can be seen on the residual plot (inset to Figure 2). To support this conclusion, the fit with the 4-parameter model resulted in a residual sum-of-squared deviation equal to 0.00111 ($RSS_1$), whereas a fit with the 5-parameter model gave a residual sum-of-squared deviation equal to 0.000332 ($RSS_2$). According to eq 3, the quotient $Q$ is equal to 28.16 and is much larger than the $F$-statistic for a probability of 99.5% [$F(1,12) = 11.75$]. Therefore, with a probability greater than 99.5%, we can conclude that the 5-parameter model is better at describing our data. Deletion of the two highest pyruvate concentration points from the fit (i.e., using 0−25 mM pyruvate) did not change the result: $RSS_1 = 5.12e{-}4$ and $RSS_2 = 3.30e{-}4$; the quotient is equal to 5.48, sufficient to allow us to conclude with 95% confidence [$F(1,10) = 4.96$] that the 5-parameter model is better at fitting the data.

Table 2: Comparison of the Pyruvate-Dependent Acetaldehyde- and Acetoin-Forming Activities by the D28A Variant

| | product assayed | |
|---|---|---|
| | acetaldehyde | acetoin |
| $V_{max}$ (units/mg) | 0.0585 ± 0.0049 | 0.230 ± 0.011 |
| $V_f$ (units/mg) | 0.0132 ± 0.0004 | 0.0465 ± 0.0044 |
| $S_{0.5}$ (mM) | 1.50 ± 0.113 | 0.956 ± 0.0554 |
| $n_H$ | 2.17 ± 0.108 | 1.87 ± 0.101 |
| $K_i$ (mM) | 3.75 ± 0.665 | 12.04 ± 2.07 |

Table 3: Effect of Acetaldehyde on Pyruvate-Dependent Acetolactate Formation by the D28A Variant

| | no acetaldehyde added | 200 mM acetaldehyde added |
|---|---|---|
| $V_{max}$ (units/mg) | 0.052 ± 0.0019 | 0.041 ± 0.00021 |
| $S_{0.5}$ (mM) | 3.24 ± 0.31 | 10.07 ± 0.11 |
| $n_H$ | 1.97 ± 0.31 | 2.10 ± 0.037 |

The corresponding values of $RSS_1$, $RSS_2$, and $Q$ for acetoin formation by the D28A variant (presented in Figure 3A) are 0.000637, 0.000106, and 55.086, respectively, with the $F$-parameter value for the 99.5% confidence interval equal to [$F(1,11) = 12.23$]. The corresponding values for acetaldehyde formation by the D28A variant (see Figure 3A) are 9.90e−5, 3.69e−6, and 465.57, respectively. The latter is much larger than the $F$-parameter for 99.5% confidence [$F(1,18) = 10.22$]. This once again affirms with a greater than 99.5% confidence that the activity of the enzyme fully saturated with pyruvate is nonzero.

The only feature readily available for estimation of the effect of the acetaldehyde product on the catalytic properties of the enzyme was acetolactate formation, produced only by the D28 variants, since this reaction did not utilize or produce acetaldehyde. The D28A variant exhibited inhibition of acetolactate formation in the presence of 200 mM acetaldehyde (Figure 3B). This inhibition resulted in a 3-fold increase of $S_{0.5}$ and only a 20% decrease in $V_{max}$ (see Table 3). The Hill coefficient did not change significantly.

*Effect of Pyruvamide on Acetaldehyde Formation by YPDC Variants.* Addition of pyruvamide (82 mM) to the E477Q variant at pH 7.5 resulted in a decrease of both the Hill coefficient and $S_{0.5}$ (Figure 4 and Table 4). The calculated value of $V_{max}$ did not change, although the observed rate at high pyruvate concentration was significantly lower in the presence of pyruvamide than in its absence.

In the presence of 83 mM pyruvamide, the pyruvate-dependent rate of acetaldehyde formation by the D28N variant exhibited dramatic changes at pH 6.0 (Figure 5), different from that expected from the behavior of wild-type and E477Q variant YPDC. Modest activation was noticed

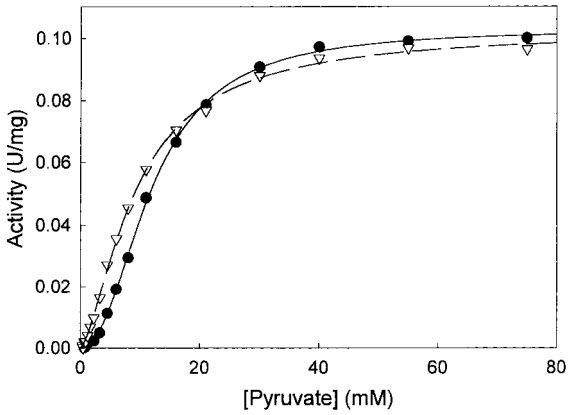


FIGURE 4: Effect of pyruvamide on the activity of the E477Q variant at pH 7.5. Conditions were as in Figure 1, except that acetaldehyde formation was estimated in the absence (closed circles) and in the presence (open triangles) of pyruvamide (82 mM). The light path was 0.514 cm; NADH and ADH were added to concentrations of 0.3 mM and 51 units/mL, respectively. The reaction was started by the addition of the E477Q variant (to a final concentration of 0.272 mg/mL, diluted into 20 mM MES, pH 6.0, 1 mM ThDP, 5 mM $MgCl_2$). Solid and dashed lines represent the best fit of the data to the Hill equation with the resulting parameters listed in Table 4.

Table 4: Kinetic Parameters for Pyruvate-Dependent Activity of the E477Q Variant in the Absence and Presence of Pyruvamide

| kinetic parameters | no pyruvamide added | in presence of 82 mM pyruvamide |
|---|---|---|
| $V_{max}$ (units/mg) | 0.103 ± 7.3e−4 | 0.102 ± 1.11e−3 |
| $S_{0.5}$ (mM) | 11.88 ± 0.152 | 9.28 ± 0.222 |
| $n_H$ | 2.18 ± 0.046 | 1.51 ± 0.039 |

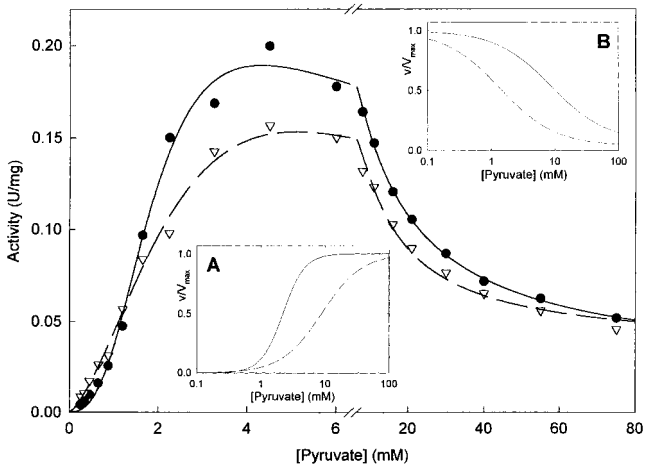


FIGURE 5: Effect of pyruvamide on the pyruvate-dependent rate of the D28N variant. Conditions were the same as in Figure 4, except the pH was 6.0 and the D28N variant was utilized. Acetaldehyde production is measured in the absence (closed circles) and the presence (open triangles) of 83 mM pyruvamide. Curves represent the best fit with the parameters shown in Table 5. Inset A shows the activating part of the pyruvate-dependent rate, and inset B shows the inhibitory part of the substrate-dependent rate. Curves for insets were calculated according to the parameters in Table 5 with the solid curve representing enzyme in the absence and the dashed line in the presence of pyruvamide.

at low pyruvate concentration. The optimal activity observed for the mid-concentration range of pyruvate (3−5 mM) decreased on addition of pyruvamide. The limiting activity ($V_f$) at saturating pyruvate concentration did not change.

Table 5: Kinetic Parameters for Pyruvate-Dependent Activity of the D28N Variant in the Absence and Presence of Pyruvamide

| | | in presence of 83 mM pyruvamide | |
|---|---|---|---|
| kinetic parameters | no pyruvamide added[a] | 5-parameter fit[a] | 4-parameter fit[b] |
| $V_{max}$ (units/mg) | 0.305 ± 0.0314 | 0.918 ± 1.014 (0.918)[b] | (0.305) |
| $V_{S\to\infty}$ (units/mg) | 0.0235 ± 0.0071 | 0.0352 ± 0.0046 (0.0352 ± 0.0031)[b] | 0.0253 ± 0.0044 |
| $S_{0.5}$ (mM) | 2.18 ± 0.18 | 8.74 ± 9.20 (8.74 ± 0.60)[b] | 2.89 ± 0.099 |
| $n_H$ | 2.56 ± 0.194 | 1.373 ± 0.142 (1.373 ± 0.058)[b] | 1.677 ± 0.081 |
| $K_i$ (mM) | 8.55 ± 2.17 | 1.36 ± 1.75 (1.36 ± 0.085)[b] | 6.47 ± 0.503 |

[a] The data were fitted to eq 2 with all parameters relaxed. [b] The data were fitted to eq 2 with $V_{max}$ fixed to the value shown in parentheses.

As summarized in Table 5, the Hill coefficient and $K_i$ both decreased, while $S_{0.5}$ significantly increased in the presence of pyruvamide. As a consequence of the decrease in $K_i$ and increase in $S_{0.5}$, the values of $V_{max}$, $S_{0.5}$, and $K_i$ became too interdependent during the fit, resulting in higher standard deviations of the calculated parameters. Fixing one of the parameters ($V_{max}$, $S_{0.5}$, or $K_i$) during the fit to the predicted value shown in Table 5 significantly decreased the standard deviations in the remaining parameters. To separate the activating and inhibitory effects of pyruvamide, the expected curves were calculated for the activation in the absence of inhibition (based on the fitting results, see inset A to Figure 5), and for the inhibition of fully activated enzyme (inset B to Figure 5). Dramatic changes are seen on the half-saturation of both activating and inhibitory slopes. Since pyruvamide addition did not change the $V_{max}$ either of WT YPDC (*4*) or of the E477Q variant, it was assumed that the D28N variant would exhibit parallel behavior. Although there was a large standard deviation in the value of $V_{max}$ in the presence of pyruvamide for the D28N variant, it was significantly different from the value in the absence of pyruvamide. The residual sum-of-squares for the fit with the 5-parameter equation (eq 2) was 0.000343; when the $V_{max}$ value was fixed at 0.305 (i.e., to the $V_{max}$ in the pyruvamide-free experiment), the residual sum-of-squares was equal to 0.000426. This resulted in a quotient (eq 3) of 4.786, supporting the notion that within 95% confidence limits the 5-parameter model is better than the model with $V_{max}$ fixed at 0.305 [$F(1,20) = 4.35$]. However, for further considerations, the value of $V_{max}$ was unimportant, since the trend of change in parameters is preserved irrespective of the value of $V_{max}$ chosen (Table 5).

Importantly for further interpretation, in the presence of pyruvamide, the Hill coefficient was in the range of 1.5−1.7 for both E477Q and D28N variants, signaling that at least two pyruvate binding sites remained vacant even at 80 mM concentration of activator.

## DISCUSSION

### *Successes and Limitations of the Current (SHS) Model*

To appreciate the need for changes in the SHS model for YPDC (*5*, *6*), its limitations need to be considered. The principal points of the model include the constitutive activation by substrate at the regulatory site, prior to binding

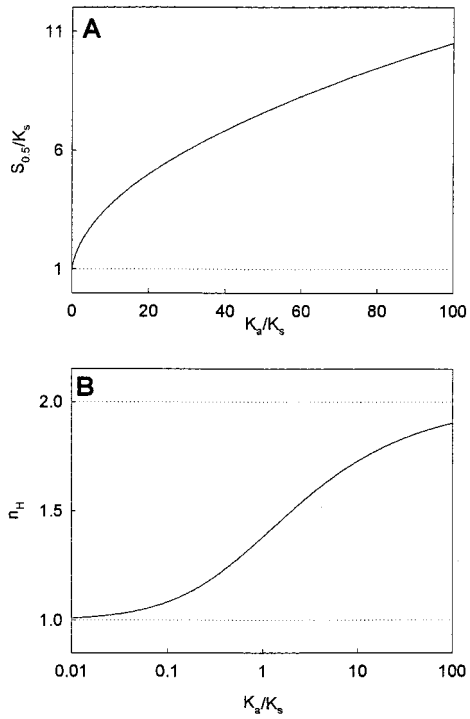


FIGURE 6: Predictions of the SHS model. Predicted values of half-saturation activity (A) and Hill coefficient (B) calculated from the equations (A11 and A12) derived in the Appendix. Limiting values of $S_{0.5} = K_s$ and $n_H = 1$ and $n_H = 2$ are shown as dotted lines for reference.

of substrate and catalytic turnover at the catalytic site. A third substrate binding site, one that can be saturated only after the first irreversible reaction, is responsible for full inhibition of the enzyme (as seen in Scheme 1 and Figure 7A). As a consequence, in the numerator of the rate equation only doubly liganded enzyme species are present, whereas in the denominator all enzyme species are present, from unliganded through triply liganded (see eq A1 in the Appendix). We utilize an equation equivalent to the one proposed by SHS, written, however, in the Adair format (*17*):

$$v = \frac{V_{max}[S]^2}{K_a K_s + K_s[S] + [S]^2(1 + [S]/K_i)} \qquad (5)$$

This form of the SHS equation clearly differentiates binding in the regulatory site from binding and catalysis in the active site. As seen in the Appendix (eq A5), the kinetic dissociation constant $K_a$ represents a combination of rate constants only responsible for regulatory site binding and the resulting activation step. At the same time, $K_s$ combines all steps starting with activation and terminating with product release. In the SHS formalism, $K_a$ is equal to $A/B$ and $K_s$ is equal to $B$ (eq A4). As shown in the next paragraph, it is the ratio of $K_a/K_s$ that determines the value of the Hill coefficient ($n_H$) and the half-saturation concentration ($S_{0.5}$). In the SHS formalism, this ratio is represented by $A/B^2$.

To understand why sometimes the SHS treatment could not describe the data, the Hill equation was utilized, and the parameters of the Hill equation were expressed in terms of the SHS parameters (see eqs A8−A12 of the Appendix for the derivation of these equations).

The half-saturation concentration has a lower limit equal to $K_s$ but has no upper limit (see Figure 6A and eq A11 of the corresponding section in the Appendix). Since binding must take place at two sites, but with only doubly liganded enzyme being active, the Hill coefficient is limited to the range between 1.0 and 2.0 (Figure 6B and eq A12), *and only positive cooperativity is expected*.

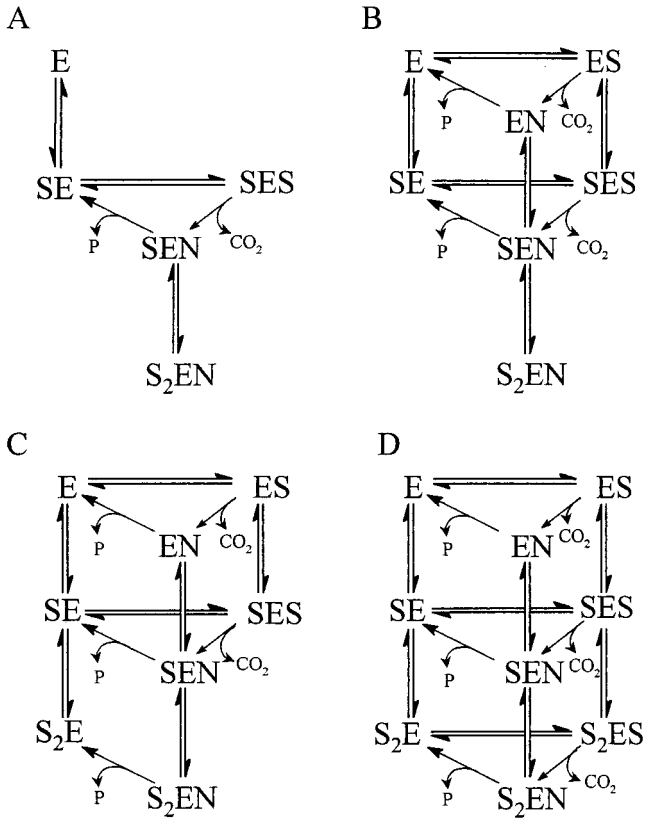


FIGURE 7: Evolution of the steady-state phenomenological model. Part A shows the SHS model. Part B shows extension of the model to include the activity of non-substrate-activated enzyme. Part C shows extension of the model to account for inhibition of the D28 variants. Part D shows an unrestricted three-site model to account for the properties of the E477Q variant. For clarity, substrate added to the different enzyme forms is not included.

It is instructive to estimate what values of the rate constants would lead to the low and high limits of the Hill coefficient, based on the equations derived in the Appendix correlating the parameters of the Hill equation and the rate constants of the SHS model. For the Hill coefficient to equal unity, the value of the ratio $K_a/K_s$ must approach zero (eq A12), only possible if one of the rate constants among $k_{a2}$, $k_{a3}$, $k_{a4}$, or $k_{c1}$ becomes negligibly small. The first three rate constants reflect the properties of the regulatory site and would not be expected to change as a result of alteration in the active site. If $k_{c1}$ is made equal to zero, then, as a consequence, $K_s$ (i.e., $S_{0.5}$ or simply $K_m$ since $n_H$ is unity) must approach $+\infty$, unless it is matched by an equally negligible $k_{c5}$ (eq A4). At the same time, since $k_{c5}$ is present in the denominator of the $K_a/K_s$ ratio, it would nullify the effect of the negligibly small $k_{c1}$ (eq A6). Therefore, it is difficult to explain how any change in the active site would result in the Hill coefficient equal to, or tending to, 1.0.

For the Hill coefficient to equal 2.0, the ratio $K_a/K_s$ must approach $+\infty$. This requires that either $k_{a1}$ or $k_{c5}$ must equal zero (eq A12). The first rate constant is involved in binding in the regulatory site; hence, it is not expected to change as a result of alteration of the active site. Even if this were

possible, it would mean that at this pH in the first case $S_{0.5} \approx A^{1/2}$ approaches $+\infty$ (unless it is matched by negligibly small $k_{c5}$). If $k_{c5}$ is negligibly small, on the other hand, then $V_{max}$ is expected to become equal to zero.

Another major consequence of the model is that the activity of the fully inhibited enzyme is predicted to be equal to zero. This property is a consequence of the presence of substrate concentration to the third order in the denominator but only to the second order in the numerator.

*The Kinetic Behavior of the Wild-Type YPDC Is Well Accounted for with the SHS Model.* We have isolated two phenomenological binding steps and deduced kinetic constants $K_a$ and $K_s$ with the Adair-type equation. In terms of the Adair equation for two binding sites, $K_a = 1.12 \pm 0.35$ mM and $K_s = 0.46 \pm 0.087$ mM at pH 6.0. The change in the Hill equation due to a change in pH can be explained with a decrease of the ratio $K_a/K_s$. For example, at pH 5.1, the expected values of the Adair parameters are $K_a = 0.35 \pm 0.20$ mM and $K_s = 0.68 \pm 0.15$ mM, and for pH 6.9, the corresponding values are $K_a = 1.03 \pm 0.36$ mM and $K_s = 3.02 \pm 0.41$ mM. Therefore, the effect of pH on $K_a$ is noticed in the pH range of 5.1−6.0, whereas an effect of pH on $K_s$ is observed by changing the pH from 6.0 to 6.9. As a first approximation, the kinetic dissociation constants reflect the distribution of enzyme among species with different number of bound substrate, product, or intermediate molecules. This implies that if the assumptions of the SHS model are correct, then the steady-state distribution of the activated versus nonactivated enzyme species changes below pH 6.0, and remains unchanged above pH 6.0. At the same time, the distribution between free and substrate- or intermediate-bound activated enzyme molecules changes above pH 6.0, but remains unchanged below pH 6.0.

*Hyperbolic $v_0$−[S] Behavior of the E477Q Variant at Low pH.* At pH ≤5.1, the E477Q variant exhibited no cooperativity (i.e., the Hill coefficient = 1.0). As discussed above, there are two likely explanations for this observation. First, the dissociation constant $K_a$ at the regulatory site (i.e., $k_{a2}$ and/or $k_{a4}$) approaches zero or is at least much smaller than the dissociation constant $K_s$ for the active site. This would ensure that for virtually any substrate concentration the regulatory site will be saturated, providing that the substrate concentration exceeds the enzyme concentration, thus resulting in an apparent hyperbolic substrate dependence. For this explanation to be correct, the information resulting from substitution at E477 would have to be transmitted to the regulatory site some 25−30 Å away, an unlikely scenario in terms of the SHS model.

The second explanation for the Hill coefficient equaling unity assumes that $k_{c1}$ (see Scheme 1 and eq A6) is almost zero for the E477Q variant at pH 5.1. This, however, would result in the reciprocal increase of $K_s$ (see eq A4 in the Appendix). One might argue that with the unavoidable error in the Hill coefficient it is difficult to differentiate a Hill coefficient of 1.0 from 1.1. Indeed, the standard error of the Hill coefficient at pH 5.1 for the E477Q variant is equal to 0.1 (as seen in Table 1). However, even after taking into consideration the error in the parameter, for the Hill coefficient to change from 1.67 at pH 6.0 to 1.1 at pH 5.1 (Table 1), the ratio $K_a/K_s$ must decrease from 6 to 0.12, i.e., 50-fold. Utilizing the values of $S_{0.5}$ for the two pH values, one would expect $K_a$ and $K_s$, respectively, of 5.8 and 0.95 mM at pH 6.0, and 0.1 and 0.833 mM at pH 5.1. Therefore, a 58-fold decrease is expected in the $K_a$ parameter, whereas $K_s$ should not change. Comparison with the values deduced for WT YPDC leads to the conclusion that, assuming that the SHS model is sufficient for all conditions and variants, the major effect of the E477Q substitution is expected to be on the activation pathway, rather than on the catalytic pathway. Once again, this supports the argument that the changes of the cooperative behavior of the E477Q variant on decreasing the pH from 6.0 to 5.1 cannot be accounted for by the SHS model.

On the basis of these arguments, we are compelled to conclude that *at pH 5.1 the E477Q variant represents nonactivated* (in SHS terms) YPDC, or a mixture of nonactivated and activated species (see section "*Justification for the Equations Utilized To Interpret Data for YPDC*"). Thus, the kinetic model must be extended to include the activity of the nonactivated enzyme, this in turn resulting in the second catalytic cycle in the scheme, originating and terminating with nonliganded enzyme (see Scheme 2 and Figure 7B). Mathematically, this means that the numerator has an additional term, first order in substrate concentration:

$$v = \frac{A_1[S] + A_2[S]^2}{B_0 + B_1[S] + [S]^2} \qquad (6)$$

This equation can account for either positive or negative cooperativity, as well as for substrate inhibition (*16*). It is possible that under most conditions (no substitution at C221 and neutral pH), the equilibrium is shifted so that the activated form has the higher activity. As will be discussed in the section "*Justification for the Equations Utilized To Interpret Data for YPDC*", not surprisingly, having present nonactivated enzyme with lower activity would still result in kinetics indistinguishable from the SHS model.

There is a possible caveat. If there is an irreversible step, such as decarboxylation, or a quasi-irreversible step with a very slow reverse rate separating the activation phase and the catalytic cycle (thereby locking the enzyme in the activated state), this could result in the invisibility of the activation phase in the steady-state kinetics. Indeed, if the enzyme is irreversibly activated, it would produce transient kinetics similar to those observed with the wild-type YPDC, but in the steady-state kinetics it will only reflect steps that follow the irreversible step. For the moment, we note that activation of YPDC in the SHS model lacks irreversibility, both chemical and phenomenological (in terms of enzyme−substrate species), thus reinforcing the conclusion that the observations with the E477Q variant at low pH cannot be explained in terms of the SHS model.

The conclusion that nonactivated enzyme is active is supported by recent data with regulatory site variants (substitutions at C221) which exhibit no substrate activation in the transient and steady-state kinetics (*18*, *19*). In addition, some of the C221-substituted YPDC variants exhibited negative cooperativity and a Hill coefficient distinctly smaller than 1 (see the C221S and C221S/C222S variants in refs *20*−*22*). These observations cannot be explained with the SHS model, which predicts the Hill coefficient to be bracketed between 1.0 and 2.0. Once we accept the notion that nonactivated enzyme is active, and it may indeed coexist

with activated enzyme, and that under some conditions it is even the predominant form of YPDC (e.g., pH, certain substitutions at the active or regulatory site residues, or substrate concentration), this form of the enzyme could also account for a Hill coefficient $\leq 1.0$.

*Partial Substrate Inhibition of the D28 YPDC Variants.* Among all of the variants studied so far in our laboratories, the D28A and D28N variants have very distinctive features. They exhibit a high degree of positive cooperativity with a Hill coefficient of 1.9−2.2 (in some cases as high as 2.5; see Table 5), depending on the product being monitored and the particular variant. They are also very sensitive to inhibition by substrate and are characterized by kinetic inhibition constants $K_i$ comparable to the half-saturation concentration $S_{0.5}$. Due to this behavior, full saturation with substrate for both activating and inhibitory sites could be achieved at reasonably low pyruvate concentrations. At full saturation with pyruvate, the calculated "final" activity $V_f$ (to differentiate it from "maximal velocity" $V_{max}$) is not equal to, but is rather distinctly greater than zero (Figures 2 and 3A). This indicates that the enzyme species with the highest number of substrate molecules bound (at least 3) is active, although its activity is lower than that of the species with the intermediate number of substrate molecules bound. This would require further modification of the kinetic model by assigning activity to the triply liganded enzyme ($S_2EN$). However, the release of the product by the $S_2EN$ enzyme species will produce doubly liganded enzyme molecules ($S_2E$), distinct from that already included in the scheme (SES), since in the former the two substrate molecules are bound in the regulatory and inhibitory sites, whereas in the latter they occupy the regulatory and the active sites. Therefore, the SHS model must be augmented by the addition of at least one intermediate and one catalytic step leading to it (Figure 7C). Mathematically, this means that both the numerator and the denominator of the rate equation will have substrate concentration to the same exponent.

Although under some particular limits eq 6 can exhibit positive cooperativity with substrate inhibition, there are insufficient degrees of freedom present in the equation to account for a Hill coefficient $\geq 2.0$, and inhibition with nonzero activity upon full saturation with substrate, as observed with the D28 variants. To describe the behavior of the D28 variant, an equation of the type shown in eq 7 will need to be used:

$$v = \frac{A_1[S] + A_2[S]^2 + A_3[S]^3}{B_0 + B_1[S] + B_2[S]^2 + [S]^3} \qquad (7)$$

The presence of an additional "enzymatic site" that is distinct from the active site was postulated a long time ago by Juni (*23*), and differential sensitivity of the acetaldehyde-forming and carboligase reactions toward limited proteolysis was explained in terms of those sites (*24*, *25*). However, as was suggested in the previous paper of this series (*12*), those two sites most probably are only temporally, but not spatially, distinguishable. The distinct need for an additional pyruvate binding site arises from a detectable decrease in catalytic efficiency at high pyruvate concentration.

Several hypotheses were proposed to explain the phenomenon of substrate inhibition (*26*, *27*). As a part of the SHS model, substrate inhibition of YPDC was attributed to possible intervention of the carboligase side reaction. However, the data presented in the second paper of the series (*12*) suggest the following: (a) Pyruvate cannot access the same active site (in wild-type or any variants except D28A and D28N) that contains the covalent intermediate. (b) It is *acetaldehyde and not pyruvate that produces acetoin by condensation with the enamine*. Among the variants studied, only the D28 variants were able to utilize pyruvate in the carboligase reaction, resulting in the formation of acetolactate. It is tempting to think of a causative relationship between acetolactate formation and the exceptional inhibition with substrate, since both phenomena were only observed with the D28A and D28N variants. However, we believe that the extraordinary inhibition with pyruvate observed with the D28A and D28N variants is not the result of simple competition of the enamine for the electrophile (a proton or acetaldehyde or pyruvate). Instead, we suggest that acetolactate formation itself is coincidental to the inhibition; in fact, it is a consequence of this inhibition. Therefore, we address inhibition with substrate as an example of imperfect protection of the active site from untimely access of substrate, and as a general property of all variants of YPDC, but expressed more effectively with the D28A and D28N variants. As to why acetolactate formation itself cannot be the cause of substrate inhibition is explained below, while later a new model for YPDC will account for the apparent substrate inhibition.

In addition to producing acetolactate, the D28 variants also produce acetoin and acetaldehyde, depending on the particular conditions. Both acetaldehyde formation and acetoin formation were inhibited by high concentrations of pyruvate, and both activities reached nonzero values at full saturation with pyruvate (Figure 3A and Table 2). Were acetolactate formation the only reason for nonzero activity of the inhibited enzyme toward acetaldehyde formation, the same reasoning should hold for acetoin formation. One could imagine that pyruvate and a proton would be competing electrophiles for the enamine, yet they need not interfere with each other's binding. Hence, even in the presence of an inhibitory pyruvate molecule, the rate of acetaldehyde release may not be zero. On the other hand, a nonzero activity of acetoin production at saturation with pyruvate means that the same logic should apply to this pathway as well. In this case, the inhibitory pyruvate and acetaldehyde must be bound to the same active site at the same time and therefore the microscopic sites of pyruvate and acetaldehyde binding must be different.

At the same time, most of our data on the mechanism of the carboligase reactions, including the stereochemical control of acetoin and acetolactate production, suggest that the acetaldehyde utilized for acetoin formation and the second pyruvate needed for acetolactate formation share the same binding site inside the active site. Indeed, the preferential synthesis of (*S*)-acetolactate and (*R*)-acetoin shows that both molecules are bound in the same orientation dictated by the size of the substituents. Addition of 200 mM acetaldehyde decreased the affinity for pyruvate 3-fold in acetolactate production, but changed the rate with saturating pyruvate concentration by only 20% (Figure 3B and Table 3). This points out that the second catalytic pyruvate molecule (involved in acetolactate synthesis) and acetaldehyde likely

compete for the same binding site if they occupy the active site of the same subunit. Were the same molecule of pyruvate involved in inhibition and acetolactate synthesis, inhibition with pyruvate should result in zero acetoin-forming activity at full saturation, since in this case pyruvate should displace acetaldehyde from the active site, thus completely shutting off acetoin formation.

On the basis of the sum of the observations, we strongly favor pyruvate expressing its inhibitory influence via a change in rate-limiting step, rather than by simple competition of the two side reactions. And the only difference between substrate inhibition of the D28A or D28N variants compared to other variants and to WT YPDC is the increased sensitivity of the D28-substituted variants toward the inhibitory substrate molecule. In the particular case of the D28A or D28N variants, an additional source of inhibition might be observed due to pyruvate-dependent diversion of the reaction to acetolactate formation.

*Enhanced Cooperativity of the E477Q Variant at Higher pH Values.* With increasing pH, the Hill coefficient ($n_H$) for pyruvate-dependent acetaldehyde formation by the E477Q variant could reach 2.5−2.6. However, the largest allowed value of the Hill coefficient within the SHS model is 2, since the number of actual binding sites sets the maximum limit achievable by the Hill coefficient. The value of the Hill coefficient rounded up to the next integer is interpreted as the minimal number of interacting sites. Therefore, for the E477Q variant at pH 7.5, the minimal number of binding sites for pyruvate is equal to 3. Mathematically, this requires an equation similar to eq 7. This similarity is not coincidental. It reflects the general feature of the D28A, D28N, and E477Q variants, namely, the existence of an additional pathway, involving an enzyme species that binds three substrate molecules concurrently, and releases the product with a rate different from other enzyme species. For the E477Q variant, the rate of the species with the maximum number of substrate molecules bound must be at least as large, or larger than any other species with a smaller number of ligand molecules, so as not to exhibit substrate inhibition. However, it is possible that both activating and inhibitory sites represent the same physical entity; for the moment, this additional site of the E477Q will be referred to as an activating site, according to its effect on the enzyme.

*Justification for the Equations Utilized To Interpret Data for YPDC.* As mentioned in the first paper of this series (*11*), the SHS kinetic model failed to explain the data for some of the variants, mostly because of the limitation imposed by the number of substrate binding sites, for some conditions too many, for some others, too few. The activation kinetics of WT YPDC were characterized at pH 6.0 (*4*), and the data analysis assumed zero activity for the nonactivated enzyme species. However, as observed in our laboratory, the C221A or C221S variants lacking the binding site for the regulatory pyruvate molecule have activity as high as 25% of WT enzyme at pH 6.0 (*18*, *20*−*22*). More recent work on the C221D and C221E variants indicated activity approaching that of WT YPDC, while the enzyme still exhibits hyperbolic kinetics (*19*). Any variant with even the slightest change in the interaction of regulatory and active sites may potentially differ from the WT enzyme in terms of activation. As an example, the E477Q variant at low pH exhibited no signs of cooperativity in steady-state kinetics.

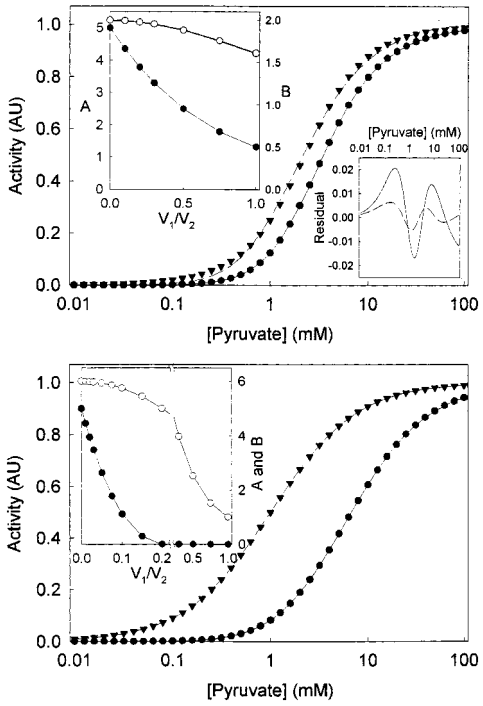


FIGURE 8: Simulation of data with eq 4. Parameters were as follows. Upper panel: $K_a = 5$, $K_s = 1$, $K_{s'} = 5$. Lower panel: $K_a = 5$, $K_s = 1$, $K_{s'} = 1$. In both panels, $V_1 = 0$ (closed circles) and $V_1 = V_2$ (closed triangles). The insets show the change in the parameters of the SHS model: *A* (closed circles) and *B* (open circles). The lower inset in the upper panel shows the residual plot for data shown in the panel with $V_1 = V_2$ fitted with the SHS equation (solid line) and the Hill equation (dashed line).

Let us assume that YPDC follows a random binding mechanism. What are the consequences of utilizing the sequential substrate binding model to describe this enzyme? An extension of the SHS model to include the activity of nonactivated enzyme will convert it to the form in Scheme 2, already discussed under Experimental Procedures. Equation 4 was also derived in the above-mentioned section.

If the activity of nonactivated enzyme $V_1$ is equal to zero, then the form of the SHS equation is unaltered. As before, the parameter *A* is equal to $K_aK_s$. However, parameter *B* is now equal to ($K_s + K_aK_s/K_{s'}$), and, therefore, parameter *B* always overestimates $K_s$ by a factor of $K_aK_s/K_{s'}$. Consequently, if the SHS equation is used to fit the data, then the constant *A* will correctly reflect the changes that take place starting with the first substrate binding step. At the same time, parameter *B* is not a simple composite of rate constants relevant only to the activated enzyme form anymore; rather, it is a composite of three dissociation constants. As a result, the parameter *V/A* will not change, whereas *V/B* will be smaller in the regime where substrate binding to the active site may precede its binding to the regulatory site.

On the basis of our data for the E477Q variant at low pH, and previously reported data for the regulatory site variants, we concluded that the activity of nonactivated enzyme $V_1$ is greater than zero. If data for such behavior are fitted to the SHS equation, then the constants *A* and *B* will both be influenced by this activity. Depending on the values of the parameters, one may expect negative, zero, or positive cooperativity (with Hill coefficient $\leq 2$), and inhibition with substrate (*16*). The overall shape of the curve will be preserved (Figure 8), and no inhibition will be observed if

$V_2/V_1 > K_a/(K_a + K_{s'})$. However, the values of the *A* and *B* parameters will have different sensitivity to the values of $V_1$ (see insets to Figure 8). Parameter *A* is much more sensitive to the values of $V_1$, since both of them describe enzyme at low concentration of substrate. If the ratio $V_1/V_2$ is changed as a function of changing conditions, such as pH, then the parameter *A* is the first one to reflect those changes. The presence of the term with nonzero $V_1$ will influence the values of the parameters of the Hill equation as well. When the curves in Figure 8 were analyzed with the Hill equation, the change of $V_1$ from zero to $V_2$ resulted in a decrease of both $S_{0.5}$ and $n_H$. The half-saturation substrate concentration changed from 3.42 to 2.21 (upper panel) and from 6.45 to 1.00 (lower panel), whereas the Hill coefficient changed from 1.50 to 1.35 (upper panel) and from 1.216 to 1.00 (lower panel). Some curves were poorly described in terms of the SHS model (see $V_1 = V_2$ curve in the upper panel of Figure 8). The SHS model, due to its asymmetric character, and requiring binding in two sites and displaying activity originating only from a single site, cannot handle the data that are more symmetric by virtue of equal activity of singly and doubly bound enzyme species. The Hill equation, due to its intrinsic flexibility, could accommodate the data more easily. This is evident from the insets in the upper panel of Figure 8, where a residual plot is presented for the SHS and Hill equations for a set of simulated data. The corresponding residual sum of squares were equal to 0.0052 and 0.00050, respectively.

Another parameter that may influence the catalytic throughput of nonactivated enzyme is $K_{s'}$, which determines the concentration of this enzyme form. As an example, data of Alvarez et al. (*5*, *6*) were simulated according to the SHS equation (eq A1). The values were as follows: $V_{max} = 320$ $s^{-1}$, $A = 2.73$ $mM^2$, $B = 1.37$ mM, $K_i = 264$ mM (*5*). Therefore, the expected values are $K_a = 2$ mM and $K_s = 1.37$ mM. According to the rate constants presented for particular steps in the same paper, more than 50% of the enzyme would exist in the nonactivated form below 0.5 mM pyruvate, with the ratio of nonactivated to activated enzyme decreasing with increasing pyruvate concentration. The simulated data were fitted to eq 4, adopting a rate constant of 80 $s^{-1}$ for the nonactivated enzyme (or $k_{cat}/4$ as was seen with the regulatory site variants) for different values of the kinetic dissociation constant of the active site of nonactivated enzyme $K_{s'}$ (Figure 9). As can be seen, the parameter *A* was strongly dependent on the value of $K_{s'}$, whereas parameters *B* (Figure 9) and $V_{max}$ or $K_i$ hardly changed at all (data not shown). At the same time, we recall that parameter *B* is equal to $(K_s + A/K_{s'})$, and therefore the expected $K_s$ will change from 1.37 to nearly zero upon a change in $K_{s'}$ from 100 to 1 mM. And, since under the same conditions, *A* will increase from ca. 2.73 to infinity, the actual kinetic dissociation constant $K_a$ will increase from the value of 2 to infinity. Therefore, if indeed $K_{s'}$ is quite small, the activated enzyme would be characterized by much higher actual cooperativity (since $K_a \gg K_s$), were it not for the unaccounted activity of nonactivated enzyme.

A serious limitation of the SHS model is in dealing with more than two pyruvate binding sites. In practice, values of the Hill coefficient $\geq 2$ may result even with the SHS model. The necessary conditions are: $K_s \ll S_{max}$ (upper limit of substrate concentration) $\ll K_a < K_i$. The condition $K_s \ll K_a$ will result in a Hill coefficient of approximately 2. The concurrent presence of substrate inhibition will decrease the observed rate and exhibit a steeper leveling-off for the rate at high substrate concentration. This will result in a faster rate for reaching apparent saturation with substrate, and will therefore mimic conditions observed with a higher Hill coefficient. Since $v_0$ increases with $[S]^2$ but inhibition (sensed as a decrease in $v_0$) is linear in [S], the inhibition may be masked as a result of the conditions described above. That, in turn, combined with the commonly accepted fixed weighing in the fitting procedure when using the Hill equation without explicitly taking inhibition into consideration, will generate an artificially high value for the Hill coefficient ($\approx$2.2). However, one must emphasize that the data must be fitted to the Hill equation without taking into account the inhibition component. Therefore, data for the D28A and D28N variants which lead to a Hill coefficient $>2$ and very low $K_i$ cannot be explained by this simple error in the fitting procedure.

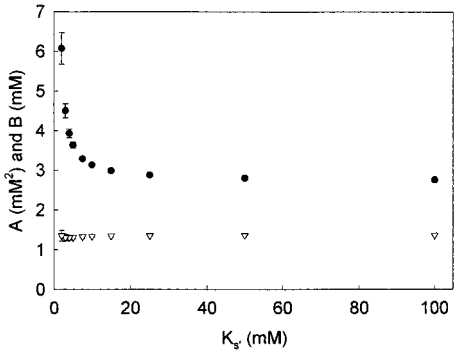


FIGURE 9: Dependence of *A* (closed circles) and *B* (open triangles) parameters of the SHS model on the value of $K_{s'}$. Data were simulated according to the SHS equation with parameters $V = 320$ $s^{-1}$, $A = 2.73$ $mM^2$, $B = 1.37$ mM, and $K_i = 264$ mM. The simulated data were fitted to the equation: $v = (V_1SA/K_{s'} + V_2S^2)/[A + BS + S^2(1 + S/K_i)]$, with $V_1 = 0.25V_2$.

Due to the uncertainty in the activity of nonactivated enzyme, and its affinity for pyruvate, as well as the variable number of pyruvate binding sites, ranging from 1 to 3, we could not utilize the SHS model to fit all of the data presented in the first paper of the series (*11*). To understand the effect of the active site substitutions on the enzyme properties, parameters of the same kinetic model must be compared. Although the Michaelis−Menten equation or eqs 6 and 7 might be utilized to characterize particular variants, none of them could describe the kinetic behavior of all the variants due to sometimes insufficient, sometimes excessive number of parameters. And, only the Hill equation could fit the experimental data for all of the variants. Since the Hill equation was not limited by any a priori assumptions concerning binding of the substrate, or the activity of any particular enzyme−substrate species, we utilized it to describe most of the data (*11*, *12*).

According to the conventional view of steady-state enzyme kinetics, the rates are partitioned into a low (*V*/*K*) and a high, or saturating, substrate concentration regime (*V*). The first parameter characterizes the conditions where substrate binding is rate-limiting and includes rate constants of all the steps starting with free enzyme up to and including the first irreversible step in catalysis. The second parameter shows catalytic potency of the enzyme saturated with substrate and

therefore represents all steps, starting with the first irreversible step, i.e., after substrate binding has occurred. With several binding steps it is difficult, if not impossible, to characterize individual rate constants involved in binding steps. In the SHS model for YPDC, the parameter *V/A* (or $V/K_aK_s$ in our representation) has similar meaning to *V/K*. It includes all steps starting with free enzyme and terminating with the first irreversible step. The meaning of *V/B* ($V/K_s$) is not well-defined due to the possible coexistence of several singly liganded enzyme species, even in the original SHS model, with obligatory occupation of the regulatory site prior to binding of substrate in the active site. The binding of the substrate to nonactivated enzyme and its nonzero activity are further complicating factors. In the former, $V/B = V/[(K_sK_a/K_{s'}) + K_s]$ would describe an averaged entity of singly liganded activated and nonactivated enzyme species. If the activity of nonactivated enzyme is nonzero, and/or there are more than two binding steps, then the apparent values of *V/A* and *V/B* would not reflect the actual events.

On the other hand, with the Hill equation, we can obtain values of $V_{max}$, $S_{0.5}$, and the Hill coefficient. To understand the meaning of different parameters of the Hill equation, one has to remember that it is based on the model:

$$E \Leftrightarrow ES \Leftrightarrow ES_2 \Leftrightarrow ... \Leftrightarrow ES_n$$

The rate expression is represented by eq 8:

$$v = \frac{V_1[S]/K_1 + V_2[S]^2/K_1K_2 + ... + V_n[S]^n/(K_1K_2...K_n)}{1 + [S]/K_1 + [S]^2/K_1K_2 + ... + [S]^n/(K_1K_2...K_n)} \quad (8)$$

The assumption is that all the enzyme−intermediate species are present at negligible concentrations except for free enzyme (E) and fully saturated enzyme($ES_n$), simplifying the rate equation to

$$v = VS^n/(S_{0.5}{}' + S^n)$$

where $S_{0.5}' = K_1K_2...K_{n-1}K_n$, and, since

$$K_1 = [E]*[S]/[ES]$$

$$K_2 = [ES]*[S]/[ES_2]$$

$$\vdots$$

$$K_{n-1} = [ES_{n-2}]*[S]/[ES_{n-1}]$$

$$K_n = [ES_{n-1}]*[S]/[ES_n]$$

and therefore

$$S_{0.5}' = [E]*[S]^n/[ES_n]$$

However, according to this definition, $S_{0.5}'$ has units of $[S]^n$. To correct this condition, usually $S_{0.5}'$ is replaced by $S_{0.5}$ with dimension of [S], leading to the simple correlation: $S_{0.5}' = (S_{0.5})^n$. The meaning of this $S_{0.5}$ is the average binding constant for a single step of substrate binding.

By analogy with *V/K* and *V/A* for very low concentration of substrate, all steps starting with the first substrate binding and terminating with the first irreversible step will be included in the parameter: $V/S_{0.5}' = V/S_{0.5}{}^n$. As with any multiple binding models, no parameter will describe the binding of a single substrate molecule. However, bearing in mind that $S_{0.5}$ represents the geometrical average of the dissociation constants of single binding steps, we can assume that $V/S_{0.5}$ will be equivalent to *V/B* and will reflect on rate constants starting from an averaged complex $ES_{n-1}$ and terminating with the first irreversible step. This approach was utilized successfully in the previous paper of the series (*11*).

### *Requirement for a YPDC Dimer as a Minimal Catalytic Unit*

In the previous sections, it was shown that some of the YPDC variants require three substrate binding steps to account for the steady-state kinetic behavior. In this section, arguments will be presented for a YPDC dimer as a minimal catalytic unit.

It is reasonable to assume that at one instant in catalysis, the regulatory site will dissociate pyruvate, and once it binds pyruvate again, it may behave as a separate binding site. Under no circumstances can the sequence of dissociation preceding the binding be reversed, since the regulatory site cannot accommodate two pyruvate molecules. It can be readily demonstrated that neither of the two scenarios (concurrent dissociation and binding, or dissociation and binding separated by the decarboxylation) can predict a Hill coefficient greater than 2.0. We learned from studies of the carboligase side reaction that with the E477Q variant, as well as with the WT YPDC, the second pyruvate cannot access the active site until the product is released. Therefore, events at neither the regulatory nor the active site can account for a Hill coefficient $>2$.

As a consequence of the above presented arguments, a separate binding site for a third pyruvate molecule, that might carry out both activation and inhibition, needs to be invoked. Could this additional binding site for pyruvate be the recently detected site (*28*) for pyruvamide binding between residues Y157 and R224? Close inspection of the binding site for pyruvamide in the molecular structure 1QPB reveals that two interactions, both involving the amido group, hold pyruvamide in place: the oxygen atom interacts with the hydroxyl group of Tyr157, and the amide NH forms a contact with the carbonyl oxygen of the main chain of Arg224. Most probably, pyruvate is ionized above pH 5.0; therefore, it would not give rise to the same interactions as pyruvamide. The carboxyl group of Asp226 is only 4 Å from the amide group, and it is most probably ionized since it has Lys327 as a neighbor, on the opposite side of the pyruvamide binding site, making it even less probable that pyruvate can bind in the same site.

We are left with no real alternative but to adopt the notion that the monomer is insufficient to describe the various issues depicted here for YPDC; hence, we extend the minimal catalytic unit of YPDC to a dimer. However, due to the character of subunit interactions, several alternatives can be envisioned for the functional dimer as the minimal catalytic unit.

The YPDC is a tetramer that represents a "dimer of dimers" structure. Two monomers depicted A and B form a tight dimer, and the two dimers form a loosely bound tetramer. The monomers in the tight dimer display some degree of asymmetry. The nonequivalence of the monomers

is further enhanced by the addition of the substrate analogue pyruvamide. In the presence of pyruvamide, one monomer in each dimer exhibited a "closed" conformation (subunit A, referred to in ref *28* as C), where the active site was essentially screened from the surroundings by two interacting loops (residues 104−113 and 290−304) from neighboring subunits of the dimer and these loops created a lid over the active site. At the same time, the second active site (in subunit B, referred to in ref *28* as O) was accessible to solvent. The two dimers displayed a remarkable degree of symmetry to one another, interacting through the interfaces created by the subunits in the same conformations.

Recently, the group that reported the novel pyruvamide binding site also suggested (*28*) that the positive cooperativity in YPDC may have nothing to do with the regulatory site, but rather it is the result of a concerted mode of action of two interacting monomers with the same conformation in each dimer. However, the model described would have all the attributes of the Monod−Wyman−Changeux scheme (*29*), along with an inability to account for inhibition by the substrate, and the negative cooperativity observed with some YPDC variants. Also, as any other two-site model, it will share the inability to account for a Hill coefficient greater than 2. It was also proposed (*28*) that only two of the four active sites are catalytically active at any point in time, leaving the remaining two "silent".

We suggest that YPDC takes advantage of the asymmetry in the tetramer with the tight dimer (hereafter called "functional dimer") being the minimal catalytic unit, possessing a total of four binding sites, two regulatory and two active sites. At the same time, if the third binding site in the case of the D28A, D28N, and E477Q variants is derived from the second subunit in the dimer (and not just a transient conformation pertinent to the post-decarboxylation active site), there is no a priori reason to restrict binding of the third pyruvate molecule to take place only after decarboxylation (as in Figure 7C). Consequently, the full scheme of three-site binding can be adopted (Figure 7D), also described by eq 7. However, as shown later, the regulation of events in one active site of the functional dimer by the state of the second active site may in fact be an integral part of the YPDC catalytic cycle. Since the dependence of steady-state kinetic behavior on pyruvate concentration did not provide any clues as to which of the three sites are utilized in the full catalytic cycle observed with the D28 and E477 variants, we utilized pyruvamide to distinguish between two possible scenarios: two regulatory and one active site versus one regulatory and two active sites being involved in the full catalytic cycle.

*Effect of Pyruvamide on the Kinetics of the E477Q Variant.* The E477Q variant in the presence of pyruvamide at pH 7.5 behaved similarly to WT YPDC. On pyruvamide addition, both the Hill coefficient and the half-saturation concentration ($S_{0.5}$) decreased (see Table 4), while the theoretical maximal velocity was unchanged. However, just as reported for WT YPDC (*4*), the observed rate at high pyruvate concentration was lower in the presence of pyruvamide. This observation cannot be explained without also invoking an inhibitory function for pyruvamide on YPDC, in addition to an activating one. Were this not the case, at no pyruvamide concentration should the activity be lower for any given concentration of pyruvate. According to the SHS sequential model, pyruvamide binds only at the regulatory site, but with lower affinity than does pyruvate, resulting in an active enzyme conformation indistinguishable from that form activated with pyruvate. It can be readily modeled that, for any concentration of pyruvate, the pyruvamide-activated enzyme should have higher activity, unless (a) $V_{max}$ is lower in the presence of pyruvamide (non- or un-competitive inhibition); or (b) the rate of substrate binding to the active site is lower and/or the dissociation rate from the active site is higher in the presence of pyruvamide, ultimately resulting in the lower affinity of the active site (competitive inhibition); or (c) a combination of both of the above (mixed inhibition).

This may prove that (a) activation by pyruvamide results in an enzyme form different from the enzyme activated by its substrate pyruvate, or (b) pyruvamide has an adverse effect on YPDC, activation mixed with inhibition. This nonequivalence of the effect of pyruvate and pyruvamide may require further modifications in the model for YPDC. Activation by pyruvate and pyruvamide may not necessarily involve the same regulatory site, once they are established to have different effects on the enzyme. Pyruvamide may also bind in additional loci, causing the inhibitory effects. We are almost certain that the recent report of a pyruvamide molecule bound in the active site of YPDC (*28*) reflects the inhibitory site for pyruvamide, rather than the pyruvate binding site. It is highly unlikely that the negatively charged pyruvate will be bound between two carboxyl groups (D28 and E477) in preference to being bound near H114 and H115, at least one of which is positively charged (*12*).

In the presence of 82 mM pyruvamide, the E477Q variant exhibited a significantly reduced Hill coefficient of 1.5 (Table 4), a value demonstrating that activated E477Q variant is more similar in its kinetic behavior to nonactivated wild-type enzyme with two binding sites than to activated WT YPDC characterized by a hyperbolic substrate dependence. Utilizing eq 4 which describes the kinetic model of two random binding sites shown in Scheme 2, the kinetic dissociation constants can be estimated for the two remaining sites. Due to the composite character of the parameter describing singly liganded enzyme species, we utilized dissociation constants calculated with the sequential model (i.e., assuming $K_{s'}$ is infinity), as was done above for WT enzyme, as initial values. The substrate dissociation constants for the sequential model are 9.5 mM for PA*ES and 4.6 mM for PA*$ES_2$. If, however, the binding is random, the value of the latter constant represents the upper limit of the dissociation constant of the high-affinity binding site (see section "*Justification for the Equations Utilized To Interpret Data for YPDC*"), since for the random binding model this parameter is equal to ($K_aK_s/K_{s'} + K_s$). If the activity of the first complex PA*ES is nonzero, then the value of $K_aK_s$ (equivalent to parameter *A* of the SHS model) will be underestimated to a greater degree than the value of $K_s$ (parameter *B* of the SHS model) (see section "*Justification for the Equations Utilized To Interpret Data for YPDC*"). Therefore, 9.5 mM will represent the lower limit of the low-affinity binding site; hence, we conclude that the kinetic dissociation constants for the E477Q variant are $\geq$9.5 and $\leq$4.6 mM.

Without additional knowledge of the activity of the singly liganded enzyme species PA*ES relative to the doubly liganded enzyme species PA*$ES_2$, we cannot make further predictions concerning the values of the constants. As

mentioned earlier, the overall shape of the curve will be preserved if $V_2/V_1 > K_a/(K_a + K_{s'})$. It is possible that $V_1$ is larger than $V_2$, providing a sufficiently high value of $K_{s'}$. If the value of $V_1$ is set equal to $V_2$ (eq 4), the constants $K_a$ and $K_s$ can reach 30 and 2 mM, respectively. For now, we cannot exclude the possibility that one of the remaining binding sites is the regulatory site from the second subunit. However, we favor an explanation where the two remaining sites represent two active sites of the functional dimer with different kinetic dissociation constants resulting from different conformations of the subunits in the functional dimer.

*Effect of Pyruvamide on the Kinetics of the D28N Variant.* In the absence of externally added activator, the D28N variant exhibited complex substrate-dependent kinetics with the activation process superimposed on the catalytic and inhibitory action of pyruvate. In an attempt to separate the three processes, the changes of the pyruvate-dependent rate of the variant were determined in the absence and presence of 83 mM pyruvamide. At low concentration of pyruvate, an increase in the pyruvate-dependent rate was noticed (Figure 5), as expected in light of the pyruvamide effect on WT YPDC and the E477Q variant. However, unexpectedly, with a further increase in pyruvate concentration, the relative activity of the variant decreased. The activity still went through a maximum, and at saturating concentration of pyruvate, it leveled off to the same value as in the absence of pyruvamide.

Therefore, pyruvamide was acting as an activator at low pyruvate concentration, and as an inhibitor at high pyruvate concentration. In the absence of pyruvamide, the Hill coefficient of the D28N variant was $\geq 2$. At least three pyruvate binding sites are needed to describe this kinetic behavior given the fact that the variant also exhibited strong substrate inhibition. The effect of pyruvamide at low pyruvate concentration is consistent with one of the sites being the regulatory site, first saturated with pyruvamide leading to an activated enzyme at all pyruvate concentrations. The adverse effect of pyruvamide at intermediate and high pyruvate concentrations requires that pyruvamide competes with pyruvate for binding in the active sites. The increase in $S_{0.5}$ shows that pyruvamide displaces the catalytic pyruvate in the active site, or that upon pyruvamide binding (activated enzyme) the enzyme has lower affinity for pyruvate. However, the latter explanation is less plausible since it is counter to the current understanding of the activation process of YPDC. Since $K_i$ decreased in the presence of pyruvamide, one can speculate that pyruvamide is assisting the inhibitory action of pyruvate. The rate at full saturation with pyruvate ($V_f$) did not change in the presence of pyruvamide, confirming that pyruvamide and pyruvate were synergistic in the inhibition of the D28N variant.

For both WT YPDC and the E477Q variant, the $V_{max}$ values remained unchanged with addition of pyruvamide. When tested with the D28N variant, within 95% confidence limit, the $V_{max} = 0.918$ unit/mg, rather than 0.305 unit/mg. However, aware of the limitation of *F*-statistics for nonlinear models, these results cannot be considered conclusive. While it is uncertain whether pyruvamide affected $V_{max}$, it did not affect $V_f$. Possibly, with the D28 variants $V_f$ carries the same functionality as does $V_{max}$ for WT and the E477Q variant.

Pyruvamide can also mimic the inhibitory mode of pyruvate, since $K_i$ for pyruvate is decreased in the presence of pyruvamide. At the same time, 82 mM pyruvamide is insufficient to saturate the inhibitory binding site, since the curve in the presence of pyruvamide still goes through a maximum, whereas 80 mM pyruvate is enough to saturate the inhibitory sites. This might be a reflection of the difference in charge of the pyruvate and pyruvamide molecules. Therefore, a positive charge in the active site might be a requirement; possibly either His114 or His115, or even both, creates the binding site for the inhibitory pyruvate.

The synergistic inhibitory effect of pyruvate and pyruvamide toward YPDC confirms once more that inhibition with substrate does not require its catalytic conversion, providing additional support to our notion that the carboligase side reaction is not responsible for the apparent inhibition even with the D28A and D28N variants.

Inhibition of the D28 variants with pyruvamide also demonstrates that pyruvate can be replaced in this role by pyruvamide, although the latter has lower affinity, as also noticed for inhibition with pyruvamide of the WT and E477Q variant. Pyruvamide inhibits those enzymes, but even at 80 mM concentration, the activity changes by only a small fraction. This similarity points to the likelihood that the origin of inhibition is the same in all enzymes discussed here. However, the presence of unaltered D28 in the WT and E477Q variant significantly reduces pyruvate access to the active site, and, as a result, protects the enzyme from inhibition by substrate. Both the E477 and D28 variants signaled the need for a third pyruvate binding site. We suggest that this additional binding site observed through steady-state kinetics is most likely the active site of the second subunit of the dimer, given the location of both substitutions.

### *A Model with Alternation of Active Sites Can Account for All Kinetic Observations*

In the previous section, a phenomenological model was presented (Figure 7D) to explain the kinetic results on some YPDC variants which imply the presence of enzyme species with three substrate molecules bound. However, the proposed model does not explain the mechanism by which YPDC performs its catalytic function. Next, a mechanistic model capable of explaining all of the observations will be proposed.

The appearance of several substrate binding sites in steady-state kinetics requires that, in addition to the mere presence of those binding sites, they must influence each other's binding or catalytic properties. The pathway of signal transduction from the regulatory site to the active site of YPDC was previously deduced in our laboratory (*18*−*22* and references cited therein). Most likely, it links two sites of the same subunit. The presence of the third binding site for pyruvate infers the existence of an additional signal transduction pathway connecting two different subunits.

The two active site acid−base residues D28 and E477 appear to be important both for catalysis and for the postulated signal transduction pathway. Variants of both D28 and E477 residues gave evidence of the presence of elevated concentration of post-decarboxylation intermediates (*12*). We propose that accumulation of those intermediates, and the unusual kinetic behavior of those variants, is the result of both a catalytic and a regulatory role of those residues. We

also believe that the kinetic peculiarities of the variants are but reflections of the complexity of the mechanism of wild-type YPDC.

The new mechanism is based on the principles exploited in an internal combustion engine. Several enzymes, most of which sustain some functional locomotion (*30, 31*), have been suggested to behave according to this model for catalysis. Recently, we utilized the same type of mechanism to explain the transient kinetic behavior of another ThDP-dependent enzyme, BFD (*10*). Substrate binding in the second active site of BFD was required for the decarboxylation of the ThDP−benzoylformic acid covalent intermediate in the first binding site.

In an internal combustion engine, the cylinders are working in an anti-concerted manner, and support each other in the transition through the maximum-energy barrier. It is the alternation of the cylinders that creates the condition in which the energy is redistributed from one cylinder to another, and the order of events is the foundation of the successful work of the engine. As we suggested earlier (*32*), the same algorithm could be utilized for the active sites of YPDC: decarboxylation in one active site may supply the energy for a second active site to bind substrate or to release product, making the sequential operation a prerequisite for normal function. If the enzyme were to utilize alternating sites, it must ensure that the environment of the active site is optimal for the designated function at each point in time. Two active sites of the functional homodimer of YPDC have different conformations. It is possible that the difference in the geometry of the active sites is a reflection of their transiently different function during catalysis.

Since D28 is within hydrogen-bonding distance from H114 or H115, its ionization state may change as a consequence of changing the distance from those residues. It is also possible that D28-COOH, being close to the covalently bound substrate−ThDP or product−ThDP adduct, may lose or gain a proton as part of the catalytic cycle. It was concluded in the second paper of this series (*12*) that D28 indeed changes its ionization state from D28-COOH to D28-$COO^-$ once the decarboxylation was completed. This could certainly ensure that the charge of the D28 residue will reflect the functional state of the active site. Therefore, we tentatively conclude that D28 and E477Q might be in the signal transduction pathway which keeps the work of alternating sites in sequence.

In brief, we suggest the following mechanism of alternating sites. Let us suppose that both active sites are catalyzing the full catalytic cycle, with a mandatory phase shift between two active sites of the functional dimer: one active site of the functional dimer is catalyzing the pre-decarboxylation phase, whereas the second subunit at the same point in time is catalyzing the post-decarboxylation phase of the reaction. Further, the coupling of the two phases of the reactions is mediated both through the prerequisite change in the conformation, and the charge/hydrogen bond pattern of the active site, as well as by thermodynamic requirements of the various steps of the reaction. Irreversibility of the decarboxylation reaction not only makes it thermodynamically favorable, but also provides a possible source of energy for the endothermic parts of the reaction, or for the shift of an unfavorable equilibrium to enhance the overall throughput of the enzyme. Alternation of sites through a conformational change would ensure the physical coupling of the two parts of the reaction.

Scheme 3

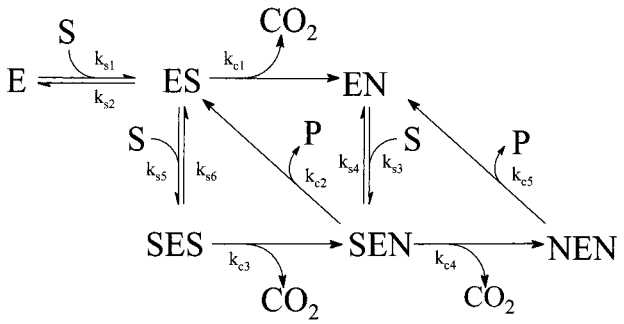


At the moment, we hesitate to assign two specific reaction steps that are coupled; however, we believe that each of them represents two phases of the overall reaction, namely, pre-decarboxylation and post-decarboxylation, as illustrated in Scheme 3. In this scheme, E represents activated enzyme, i.e., ES* in the SHS formalism, with the apparent dissociation constant of the regulatory site $K_a$, and S is free substrate. ES and EN represent one of the pre-decarboxylation (enzyme−substrate noncovalent complex or LThDP) and post-decarboxylation (enamine or HEThDP, or enzyme−product noncovalent complex) intermediates, respectively. The positioning of the letter S or N to the right or left side of the symbol for the enzyme reflects involvement of two different monomers of the functional dimer. As can be seen, the release of product is only possible after substrate binding, and possibly LThDP formation in the neighboring subunit. Some of the enzyme species (for example, ES or SEN) represent nodes (vertexes) of the graph with the choice of reactions they can undergo, and are partitioned between different pathways according to their relative kinetic efficacy. The intermediate EN is formed in an irreversible step from decarboxylation of ES. The product release is irreversible due to reduction of acetaldehyde (P) in the coupled reaction. If either of the two irreversible steps is obstructed, the accumulation of pre- or post-decarboxylation intermediates will result. Notice that for simplicity, Scheme 3 does not include catalysis by nonactivated enzyme, although this would be a logical extension of the model.

One should recall that binding steps preceding irreversible steps are invisible in the steady-state rate expression. A corollary is that the rate of steps connecting the post-irreversible-step and pre-irreversible-step pools of the enzyme in the direction opposite to the direction of the irreversible step must be negligibly slow compared to the rate of the irreversible step. This is a consequence of a broader relationship: the higher the steady-state concentration of enzyme−substrate species, the larger the effect they will have on the rate of the reaction. In the catalytic cycle of YPDC, decarboxylation is chemically irreversible. However, phenomenologically it may have features of reversible steps, if the release of the product, connecting the pool of post-decarboxylation intermediates and the pool of free activated enzyme, is fast compared with the rate of decarboxylation.

We suggest that the pH effects on the steady-state kinetics of the WT YPDC and its variants illuminate the different parts of a single mechanistic model through the changes in relative kinetic efficiency of particular steps. As illustrated

Scheme 4

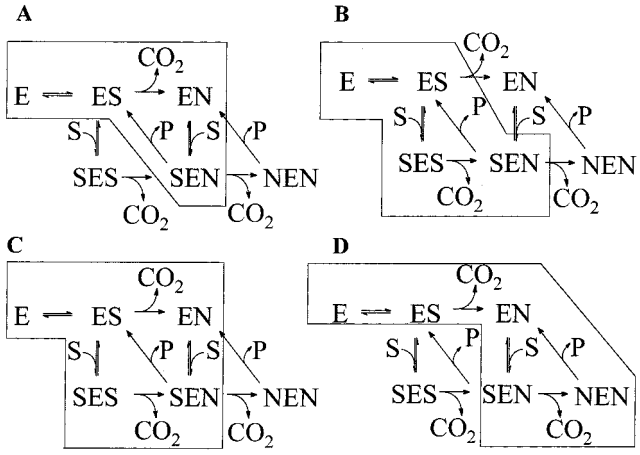


in Scheme 3, the presumed mechanistic model of the reaction represents the network of possible reversible and irreversible steps. This same model can explain the observed hyperbolic behavior, as well as the enhanced cooperativity with a Hill coefficient higher than 2. It should be noted that binding of pyruvate in the regulatory site of the second monomer of the dimer is not included in Scheme 3. Therefore, each catalytic cycle may include an additional substrate binding step for saturation of the regulatory site, a consequence being a Hill coefficient as high as 4, providing that particular conditions will favor substrate binding steps and LThDP formation of the activated enzyme over decarboxylation.

The general equation for Scheme 3 is

$$v = \frac{A_2[S]^2 + A_3[S]^3}{1 + B_1[S] + B_2[S]^2 + B_3[S]^3} \quad (9)$$

where

$$A_2 = \frac{k_{s1}k_{c1}(k_{c2} + k_{c4})}{K_a k_{s2} k_{c2}}$$

$$A_3 = \frac{k_{s1}k_{c3}k_{s5}(k_{c2} + k_{c4})}{K_a k_{s2} k_{c2}(k_{c3} + k_{s6})}$$

$$B_1 = \frac{1}{K_a} + \frac{k_{s1}k_{c1}(k_{c2} + k_{c4} + k_{s4})}{K_a k_{s2} k_{c2} k_{s3}}$$

$$B_2 = \frac{k_{s1}(k_{c1}k_{c4} + k_{c1}k_{c5} + k_{c2}k_{c5})}{K_a k_{s2} k_{c2} k_{c5}} + \frac{k_{s1}k_{c3}(k_{c4} + k_{s4})k_{s5}}{K_a k_{s2} k_{c2} k_{s3}(k_{c3} + k_{s6})}$$

$$B_3 = \frac{k_{s1}k_{s5}(k_{c2}k_{c5} + k_{c3}k_{c5} + k_{c3}k_{c4})}{K_a k_{s2} k_{c2} k_{c5}(k_{c3} + k_{s6})}$$

Depending on the predominant utilization of the three catalytic cycles in Scheme 3 (separately and in combination with one another), several scenarios of apparent enzyme kinetic behavior are possible as summarized in Scheme 4. The preferred catalytic pathway in each case is outlined with the shaded area, and eq 9 is simplified by assuming that the rate constant of the remaining steps is negligibly small, essentially zero.

Case 1 is illustrated in Scheme 4A (assuming $k_{s5} = 0$ and $k_{c4} = 0$). If the rate of product release ($k_{c2}$) from SEN is comparable to the rate of decarboxylation ($k_{c1}$) of ES, then the number of the binding steps will reflect pre-decarboxylation activation and binding. The rate equation for this situation is

$$v = \left(\frac{k_{s1}k_{c1}}{K_a k_{s2}}[S]^2\right) \Big/ \left[1 + \left(\frac{1}{K_a} + \frac{k_{s1}k_{c1}(k_{c2} + k_{s4})}{K_a k_{s2} k_{c2} k_{s3}}\right)[S] + \left(\frac{k_{s1}(k_{c1} + k_{c2})}{K_a k_{s2} k_{c2}}\right)[S]^2\right] \quad (10)$$

If the release of the product ($k_{c2}$) from SEN is slow compared to the rate of decarboxylation ($k_{c1}$) of ES, then this will lead to accumulation of post-decarboxylation intermediates, and the observed hyperbolic behavior, providing only the active site binds substrate in the catalytic cycle ES → EN → SEN. The rate equation for this condition is

$$v = \frac{k_{c2}[S]}{k_{s4}/k_{s3} + [S]} \quad (11)$$

If, however, substrate binding in the regulatory site is a required step of this cycle, then sigmoidal substrate dependence will be observed with a resulting Hill coefficient in the range of 1−2.

Case 2 is illustrated in Scheme 4B (assuming $k_{c1} = 0$, $k_{c4} = 0$, and $k_{s4} = 0$). The predominant pathway is through the cycle ES → SES → SEN. The rate equation (eq 12) will now reflect the binding of the substrate in at least three sites: regulatory ($K_a$), active ($k_{s1}$ and $k_{s2}$), and activating ($k_{s5}$ and $k_{s6}$) sites.

$$v = \left[\frac{k_{s1}k_{c3}k_{s5}[S]^3}{K_a k_{s2}(k_{c3} + k_{s6})}\right] \Big/ \left[1 + \frac{[S]}{K_a} + \frac{k_{s1}[S]^2}{K_a k_{s2}} + \frac{k_{s1}k_{s5}(k_{c2} + k_{c3})[S]^3}{K_a k_{s2} k_{c2}(k_{c3} + k_{s6})}\right] \quad (12)$$

The Hill coefficient is predicted to be greater than 2 and may reach a value as high as 4, depending on the number of regulatory sites required for the catalysis.

Case 3 is illustrated in Scheme 4C (assuming $k_{c4} = 0$). The steps from both previous cases, A and B, are present. The rate equation describing this situation is

$$v = \left[\frac{k_{s1}k_{c1}}{K_a k_{s2}}[S]^2 + \frac{k_{s1}k_{c3}k_{s5}}{K_a k_{s2}(k_{c3} + k_{s6})}[S]^3\right] \Big/ \left[1 + \left(\frac{1}{K_a} + \frac{k_{s1}k_{c1}(k_{c2} + k_{s4})}{K_a k_{s2} k_{c2} k_{s3}}\right)[S] + \left(\frac{k_{s1}(k_{c1} + k_{c2})}{K_a k_{s2} k_{c2}} + \frac{k_{s1}k_{c3}k_{s4}k_{s5}}{K_a k_{s2} k_{c2} k_{s3}(k_{c3} + k_{s6})}\right)[S]^2 + \left(\frac{k_{s1}k_{s5}(k_{c2} + k_{c3})}{K_a k_{s2} k_{c2}(k_{c3} + k_{s6})}\right)[S]^3\right] \quad (13)$$

If the rate of decarboxylation of SES ($k_{c3}$) is slower than the rate of decarboxylation of ES ($k_{c1}$), then substrate inhibition might be observed. Note that the rate at saturation with substrate is nonzero if $k_{c3}$ has nonzero values. If, on the other hand, the rate of decarboxylation of SES is faster than the rate of decarboxylation of ES, then three consecutive

substrate binding steps may be observed with apparent cooperativity somewhat lower than that of Case 2, due to a nonzero value of $k_{c1}$.

Case 4 is shown in Scheme 4D (assuming $k_{c2}$ and $k_{s5} = 0$). The rightmost catalytic cycle (EN → SEN → NEN) is separated by an irreversible step ($k_{c1}$) from enzyme activation and substrate binding in the active site of the first monomer. Due to this condition, only binding steps present post-decarboxylation are visible. This could also account for the observed activation kinetics without explicit involvement of a regulatory site. If the rate of product release from SEN ($k_{c2}$) is zero, and the rate of decarboxylation of ES ($k_{c1}$) is slower than the rate of SEN decarboxylation ($k_{c4}$), then the transient kinetics will reflect the irreversible step, decarboxylation of ES. Once ES is decarboxylated, the enzyme will utilize the right-most triangle EN−SEN−NEN as a catalytic cycle, making it plausible to have an enzyme form showing hyperbolic steady-state kinetics and transient activation. For the single binding step, as shown in the Scheme 4D, a hyperbolic $v_0$−[S] kinetic behavior would be predicted:

$$v = \frac{\frac{k_{c4}k_{c5}}{k_{c4}+k_{c5}}[S]}{\frac{(k_{c4}+k_{s4})k_{c5}}{(k_{c4}+k_{c5})k_{s3}} + [S]} \quad (14)$$

If the binding in the regulatory site is involved in this catalytic cycle, a sigmoidal substrate dependence will be predicted, with the Hill coefficient bracketed between 1 and 2.

*WT YPDC* exhibits sigmoidal substrate dependence with limited substrate inhibition at all pH values. It is relevant that each substrate binding step in Scheme 3 also includes formation of LThDP and its reversal. Therefore, if the rate of LThDP formation is slower than the rate of decarboxylation, then given the choice of whether (as in the case of ES) to undergo decarboxylation or bind substrate in the second active site, forming LThDP, and only then undergo decarboxylation, the enzyme will select the fastest branch (ES to EN). This might be the reason WT YPDC with four potential binding sites for substrate does not exhibit a Hill coefficient >2. Earlier studies (*33*) and, more recently, Chen and Huskey (*34*) demonstrated that decarboxylation is not rate-limiting for WT YPDC in the pre-decarboxylation phase ($^{13}C/^{12}C$ kinetic isotope effects on $CO_2$ release measured under *V/K* conditions). Therefore, decarboxylation must be faster than LThDP formation. This will lead to a situation where the enzyme would, for the most part, rather undergo decarboxylation of ES than substrate binding with subsequent LThDP formation, resulting in a Hill coefficient <2. At the same time, for nonzero values of $k_{s5}$, some enzyme molecules will still proceed via the pathway ES → SES → SEN with lower apparent rate, leading to the observed substrate inhibition. Observation of this inhibition implies that $k_{c3} \ll k_{c1}$; i.e., were it possible to saturate the enzyme with substrate, pyruvate present in the second active site will inhibit the enzyme.

At the present time, we cannot determine the fate of the SEN enzyme−substrate species of WT YPDC (but see section titled "*Structural Evidence Supporting Alternating Sites Reactivity*"). Two possible outcomes (Schemes 4A and 4D) would predict the same number of substrate binding sites. The major difference between them is the sequence of the two irreversible steps of decarboxylation and product release. In Case 1 (Scheme 4A), product release from one site ($k_{c2}$) precedes decarboxylation of LThDP ($k_{c1}$) in another site. The fast consumption of ES would be important for shifting the equilibrium since release of the acetaldehyde product is readily reversible. Or, it could provide the energy for substrate binding after decarboxylation. In Case 4 (Scheme 4D), product release ($k_{c5}$) follows the decarboxylation reaction ($k_{c4}$). In this situation, the decarboxylation reaction may provide energy for the subsequent product release. It is also possible that WT YPDC utilizes both pathways simultaneously, as described by the equation (eq 15):

$$v = \left[\frac{k_{s1}k_{c1}(k_{c2}+k_{c4})}{K_a k_{s2}k_{c2}}[S]^2\right] / \left[1 + \left(\frac{1}{K_a} + \frac{k_{s1}k_{c1}(k_{c2}+k_{c4}+k_{s4})}{K_a k_{s2}k_{c2}k_{s3}}\right)[S] + \left(\frac{k_{s1}(k_{c1}k_{c4}+k_{c1}k_{c5}+k_{c2}k_{c5})}{K_a k_{s2}k_{c2}k_{c5}}\right)[S]^2\right] \quad (15)$$

If the two reactions, decarboxylation and product release, were tightly coupled, then they would be performed as a single catalytic step with carbon dioxide and acetaldehyde release resulting from it. However, the transition state in this case might still be closer to either ES or NEN. Note that NEN does not necessarily represent enamine bound in two active sites of the dimer, but rather any combination of post-decarboxylation ThDP-bound covalent intermediates.

*The E477Q variant* exhibits pH-dependent behavior very different from the other variants and WT YPDC. Only a single substrate binding step was observed at pH 5.0, and the number of sequential binding steps could reach as many as 3 with increasing pH. This variant also exhibited a higher rate of decarboxylation than LThDP formation at pH 6.0 (*34*). Therefore, at least at pH 6.0, the ES enzyme species are decarboxylated predominantly to form EN (Scheme 4A). However, in the second paper of the series (*12*), we demonstrated that product release was impaired more than decarboxylation. This would convert the SEN species preferentially to NEN ($k_{c4}$), rather than release product from it ($k_{c2}$) (Scheme 4D).

It is possible that with increasing pH the relative rates of particular steps change for the E477Q variant. Perhaps, at low pH the hyperbolic $v_0$−[S] plots reflect the preponderance mostly of nonactivated enzyme. Alternatively, if the enzyme utilized Case 4, and the regulatory site does not participate in the catalytic cycle (see Scheme 4D), similar behavior may result. Of course, both scenarios may happen concurrently as well, and more detailed studies of the activation kinetics would be needed to select the more likely one at low pH for the E477Q variant. As the pH is increased, more and more enzyme molecules become activated, increasing the degree of sigmoidicity. If the rate of formation and/or decarboxylation of the SES enzyme−substrate complex is slower than the rate of decarboxylation of the ES complex, then some degree of inhibition will be in evidence as well (Scheme 4C). If, with the subsequent pH increase, the rate of formation

and/or decarboxylation of SES becomes faster than the rate of decarboxylation of ES, then a further increase of sigmoidicity will result with a Hill coefficient >2.0 (Scheme 4B). A disappearance of substrate inhibition, coincident with an increase in Hill coefficient to a value greater than 2, as seen with the E477Q variant at higher pH, might be a reflection of this transition.

*The D28 variants* exhibited a high degree of cooperativity and partial inhibition with substrate. The D28A variant undergoes rate-limiting decarboxylation in the pre-decarboxylation phase (*34*). Therefore, at least at high pyruvate concentration, this variant will predominantly utilize Case 2, as illustrated in Scheme 4B. The relative efficacies of the two branches, ES → EN → SEN and ES → SES → SEN, are proportional to $k_{c1}$ and $k_{c3}k_{s5}[S]/(k_{c3} + k_{s6})$, respectively. Therefore, at low concentration of substrate, the enzyme will proceed through the former branch (Scheme 4A). If the rate of decarboxylation of ES ($k_{c1}$) is faster than the rate of decarboxylation of SES ($k_{c3}$), then partial substrate inhibition will be observed. An additional source of inhibition of the D28 variants might arise if one more pyruvate molecule is bound to the SEN or NEN intermediates to form acetolactate.

*Pyruvamide effects* can also be explained in light of the alternating sites model. In addition to binding in the regulatory site ($K_a$), pyruvamide may also bind in the second active site of the enzyme species ES (step $k_{s5}$). This will lead to the lower catalytic turnover rate just as with inhibition by pyruvate. Pyruvamide could inhibit both wild-type and variant YPDCs by mimicking pyruvate, by forming a PA·ES complex, analogous to the SES complex in Scheme 3.

*Number of Active Sites Participating Simultaneously in the Carboligase Reactions*. As discussed in the second paper of the series (*12*), acetoin and acetaldehyde formation share steps in common through decarboxylation. On the basis of the relative rates of acetoin and acetaldehyde formation, we concluded that one of the steps, post-decarboxylation, is rate-limiting for acetaldehyde formation by the D28A, E477Q, H114F, and H115F variants. However, the apparent increase of the $V_{max}$ for acetoin formation with the E477Q and D28N variants, when compared to the WT YPDC, could not be explained. According to eq 3 in paper 2 (*12*), the rate of acetoin formation should depend equally on the rates of formation of LThDP and its decarboxylation, as well as on the rate of formation of BDThDP and acetoin release. It would be surprising to find an increase in the efficiency of the variants in steps up to and including decarboxylation. Also, the stereochemical results suggested that neither E477 nor D28 is directly involved in the formation of BDThDP, and it is the N4′-amino group of the aminopyrimidine ring that appears to be of primary importance in the formation of acetoin. Therefore, the rates of the post-decarboxylation phase of the acetoin-forming reaction would not become more efficient as a result of the substitutions.

The explanation can be found in the alternating sites mechanism, according to which WT YPDC has post-decarboxylation intermediates in approximately half of the active sites at any point in time. Since the rates of the decarboxylation and acetaldehyde release steps are believed to be equal under conditions of saturation with pyruvate (*5*, *6*), the enzyme will be present as a 1:1 ratio of pre-decarboxylation intermediates (E−pyruvate complex and LThDP) and post-decarboxylation intermediates (enamine, HEThDP, and enzyme−product complex). The rate of acetoin release was equal in the forward (*12*) and reverse reactions (the latter was measured with acetaldehyde as a sole substrate in ref *35*), attesting that in both directions all of the reactions leading to the enamine are faster than BDThDP formation and acetoin release. Therefore, the rate of acetoin formation in the presence of saturating acetaldehyde will only depend on the total concentration of post-decarboxylation intermediates.

It would appear that due to the impaired acetaldehyde release by the E477Q variant, step $k_{c4}$ will be more efficient than $k_{c2}$ and $k_{c5}$ in Scheme 3, and all four active sites of the enzyme will be occupied by the post-decarboxylation intermediates (depicted as NEN). Therefore, the effective concentration of enamine is at least twice that of the WT YPDC, explaining the higher rate of acetoin formation by the E477Q variant.

The $V_{max}$ for acetoin formation by the D28N and E477Q variants is comparable. That is, the combined concentration of enamine and HEThDP (two species that are in rapid and reversible equilibrium, see refs *36* and *37*) would be comparable in both cases if the D28N variant were not inhibited by pyruvate. Therefore, at low pyruvate concentration, all four sites in the tetramer of the D28N variant participate in the formation of acetoin, and the release of acetaldehyde is rate-limiting (*12*).

*Activation in the Alternating Active Sites Model.* The hypothesis of alternating catalytic sites reactivity is buttressed by the close contact of the subunits in the asymmetrical dimer (1YPD and 1QPB), and the striking differences between the two monomers. We believe that activation of YPDC is a necessary event to start the catalytic cycle, but may not be necessary for its perpetuation.

Certainly, the activation step cannot be a part of the catalytic cycle of the E477Q and D28N variants whose carboligase reaction was studied in the second paper (*12*). It was reported that the rate constant for the zero-order activation reaction of wild-type YPDC pursuant to substrate binding in the regulatory site is 0.5 $s^{-1}$ (*4*). Should this step be an essential part of each catalytic cycle, the turnover could not be higher than this value. For the E477Q and D28N variants, the turnover number for acetoin formation is twice this number. One can certainly expect that substitution of different amino acid residues may result in a change of the rate of the activation process. However, it is difficult to explain why substitutions at two different active site positions would lead to the same magnitude of rate enhancements. In addition, only one regulatory site is clearly visible in the steady-state kinetic behavior of the variants. Therefore, we are compelled to suggest that the activation step, which changes the enzyme from a lower to a higher activity form, is required to commence the catalytic cycle; i.e., E represents the higher activity conformation in Schemes 3 and 4. But, the higher activity conformation persists through the catalytic cycle, whether or not pyruvate remains in the regulatory binding site. The affinity of the regulatory site for the substrate/activator is likely to increase as a result of occupation of the active site. According to Scheme 2 and the law of energy conservation, the kinetic dissociation constant corresponding to the step from ES to SES (not assigned any symbol in Scheme 2) will have a value equal to $K_aK_s/K_{s'}$. That is, since $K_{s'}$ is probably larger than $K_s$, the value of

Scheme 5

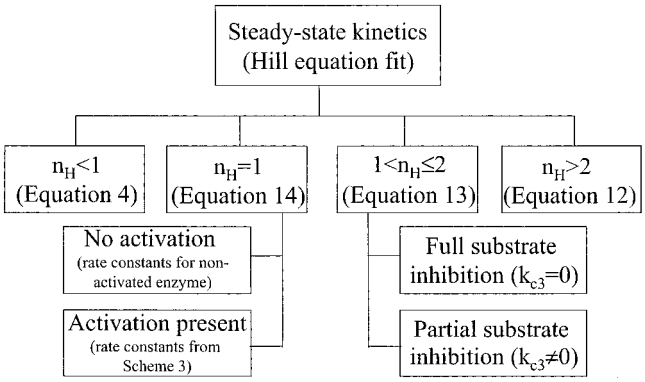


$K_aK_s/K_{s'}$ would be smaller than $K_a$. Under these conditions, for any concentration of pyruvate, the regulatory site is more likely to be occupied after the enzyme was activated, and catalytic turnover had commenced, rather than prior to initiation of activation. This is just another feature of YPDC making it a hysteretic enzyme.

One can compare nonactivated YPDC to a motionless mechanical pendulum. It will remain still until some force displaces it from this original ("ground") state. Once it was displaced, the energy supplied from the weight on the chain will sustain its constant movement until the weight reaches its lowest point. In a similar vein, activation is a necessary event, which reflects the transition from the nonactivated to the activated state. It distorts the symmetry in the dimer, creating the environment for a mechanism involving alternation of active sites. The decarboxylation reaction would supply the energy, and the turnover will continue until the substrate is depleted.

*Choice of the Steady-State Equation Utilized.* The ultimate goal of kinetic studies is to determine the rate constant for a particular step in a reaction. In the case of the alternating sites mechanism, as demonstrated above, several patterns of apparent kinetic behavior can be envisioned. All of those scenarios can be described by eq 7 and most of them (where the activity of nonactivated enzyme is negligible) by eq 9. While, in theory, one could fit the kinetic data with no apparent or low cooperativity to either eq 7 or eq 9, due to the excessive number of parameters, the calculated values will have high standard deviations. Therefore, we decided to select the rate equation according to the observed apparent steady-state behavior of the YPDC variants. We have utilized the Hill equations as a diagnostic tool; depending on the presence and degree of substrate inhibition, either the original (eq 1) or the modified Hill equation (eq 2) could be used. The value of the Hill coefficient then determines which pathway of the mechanism is predominantly utilized and which equation best describes the observed behavior (Scheme 5). Note, however, that at least in the preliminary studies, i.e., before the values of some rate or dissociation constants are determined, an equation with a form similar to eqs 6 and 7 should be utilized.

### *Structural Evidence Supporting Alternating Sites Reactivity*

Mechanistically, formation of LThDP from pyruvate and ThDP and release of acetaldehyde from HEThDP represent, in essence, reverse directions of the same reaction, the transfer of a proton to or from the C2α oxygen. These reactions are preceded by proton abstraction from C2 of the thiazolium ring, and are separated by proton donation to C2α of the enamine to form HEThDP. The latter two reactions also represent the reverse of mechanistically very similar reactions. Therefore, the sequence of reactions carried out by YPDC can be viewed as two reactions in tandem, where in the second repeat the reverse reactions are utilized. The four parts of the catalytic cycle are shown in Scheme 6, where parts 1 and 3 represent reversal of one reaction and parts 2 and 4 represent reversal of another reaction. On the basis of the principle of microscopic reversibility, it would be more efficient for the enzyme to utilize the same group for each pair of the reversed reaction. Although a priori it would not be a requirement to utilize the same group in all four reactions, an inspection of the YPDC structure suggests this to be an attractive possibility.

Scheme 6

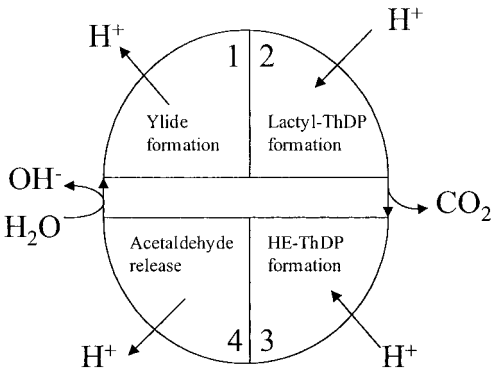


Activation perturbs YPDC from its nearly symmetrical state to a highly asymmetrical one. In each dimer of the 1YPD structure, one active site reveals a closed conformation, with the closed lid over the active site and the N4′-amino group in very close proximity to the C2 thiazolium atom.

On the basis of the structural data, we propose a model where this same N4′-amino group is responsible for all of the reactions. The choice of the candidate for this reaction should reflect easy regulation of the p$K_a$ of the group. Since only E477 and D28 of the four potential acid−base side chains are in close proximity of the C2 of the thiazolium ring, we are compelled to choose them over H114 or H115. However, on the basis of the rates of acetoin formation by their variants, D28 and E477 appear to have no significant role pre-decarboxylation. Therefore, it is more likely that neither E477 nor D28 assists ylide formation, or protonation in LThDP formation. We assume that the N4′ atom of the aminopyrimidine ring is the major player in the proton transfer in the first half of the reaction. With the V conformation enforced by several factors (*38*), it is virtually impossible to displace the amino group by several angstroms. However, in the YPDC structure (1YPD file), the beginning of a modest shift is already present (Scheme 7). In the "closed" active site (shown in the semitransparent colors), the distance between N4′ and C2 is decreased to 3.09 Å compared to 3.5 Å in the "open" active site (shown in solid colors), whereas the distance between these two atoms is the same in both active sites of nonactivated YPDC. We do not suggest that those distances be accepted as alternative limits of the movements displayed by the ThDP rings, but

Scheme 7

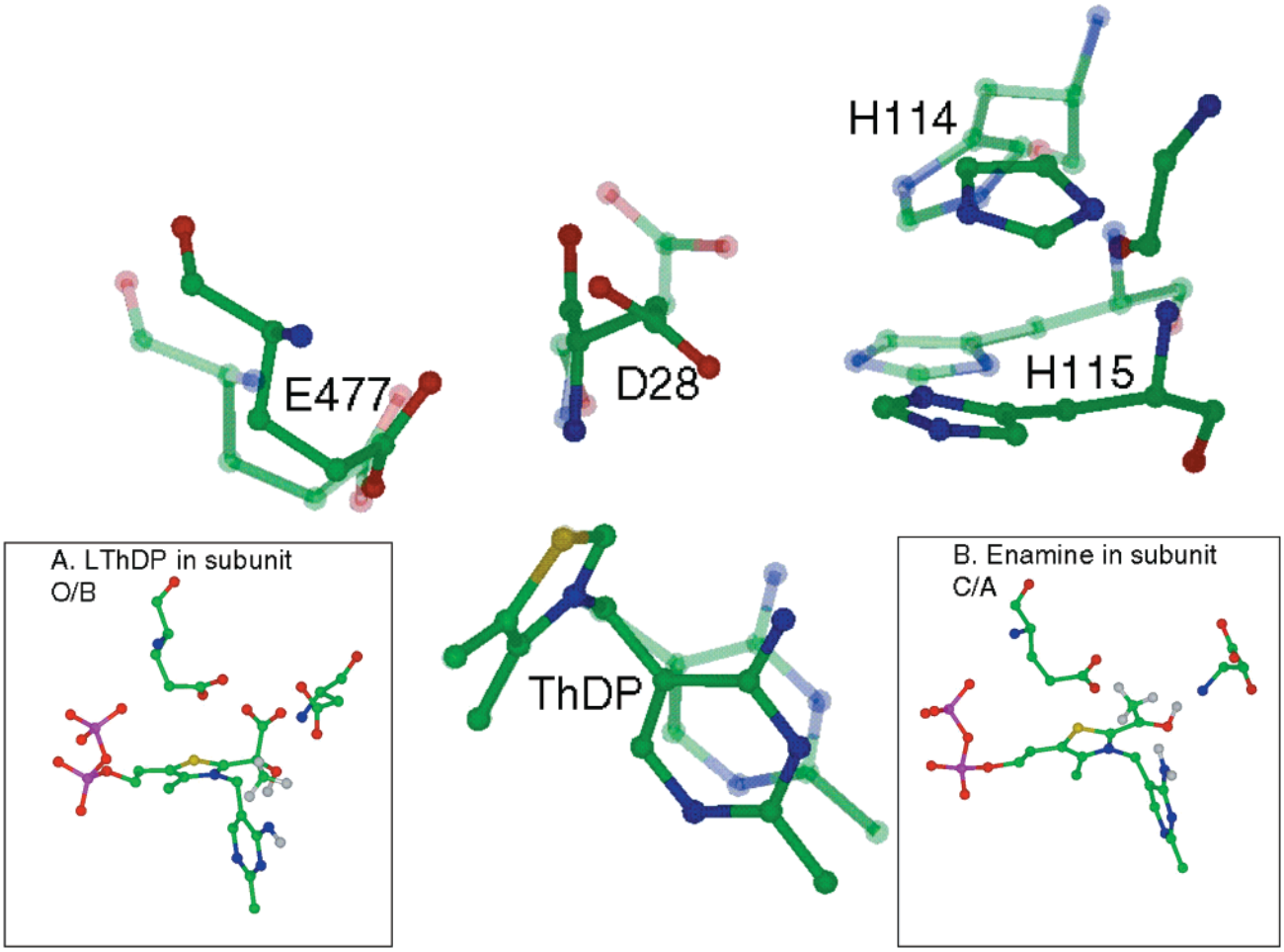


rather as an illustration that those movements are plausible. The presence of the substrate (but not its pyruvamide analogue) may further improve the geometry of the active site to adjust it for optimal functioning. The "closed" active site of the A/C subunit conformation can accommodate proton transfer from C2 to N4′, but the site is too tight to accommodate the covalently bound pyruvate of LThDP. Therefore, we suggest that the A/C conformation of the closed active site provides a working model for formation of both the ylide and HEThDP, where the N4′ atom comes within close contact with the C2 or C2α atom to donate or accept a proton (inset B in Scheme 7). In the "open" active site of the B/O subunit conformation, the N4′ atom is further from C2α and provides a model for participation of N4′ in the protonation or deprotonation of the C2α hydroxyl group in LThDP formation (inset A in Scheme 7) or acetaldehyde release.

According to this working hypothesis, D28 and E477 (as well as H114 and H115) will assist in the proton transfer providing a hydrogen relay chain. Neither the E477Q nor the D28A substitutions could change the rate of H/D exchange at C2 in the nonactivated enzyme [see paper 1 of the series (*11*)]. However, the rate of exchange in the presence of pyruvamide was 20-fold lower for those variants than for the WT YPDC, suggesting that the reaction pathways may not be identical in the activated and nonactivated enzymes. At the same time, these results also hinted at the participation in some manner of both D28 and E477 in the signal transduction pathway, leading from the regulatory or perhaps inhibitory site for pyruvamide to the active site. In the "closed" A/C active site, the nearest distance between D28 and N4′ is 6.2 Å and between D28 and E477 is 6.0 Å. In the B/O (open) subunit, the minimal distance from D28 to N4′ is 4.66 Å and from D28 to E477 is 3.51 Å, suggesting that the rate of proton transfer between N4′ and D28 and/or E477 may be enhanced in the B/O subunit. It would be important, for example, to transfer the proton to the N4′ atom once LThDP was formed to prevent the loss of pyruvate leading to reversal of the reaction. This may also be a convenient mechanism for changing the state of ionization of the D28 side chain, if D28-COOH were to donate the proton. The decarboxylation of LThDP to the enamine follows, rendering the enamine ready to accept a proton from the N4′ atom, and D28-$COO^-$ will participate in the protection of post-decarboxylation intermediates, as outlined in the second paper of the series (*12*).

Invoking the principle of microscopic reversibility, if the N4′-amino group is involved in protonation of the C2α-alkoxide of LThDP, it might also participate in the release of acetaldehyde (or acetoin), abstracting a proton from the C2α-hydroxyl group of HEThDP (BDThDP). However, it is likely that D28, H114, H115, and E477 need to assist in the latter reaction, since acetaldehyde release was impaired to a greater degree by the alteration of these active site residues than the steps preceding decarboxylation, judging by the rates of acetoin formation. Just as was reasoned for

LThDP formation, it would be important, for example, to transfer a proton from the N4′ atom once acetaldehyde is released, so as to prevent the reversal with HEThDP formation. Once again, the D28 side chain will become D28-COOH, signaling the end of the post-decarboxylation phase. And, the imino tautomer of the aminopyrimidine ring regenerated in this reaction will be ready for catalysis of the first step of the catalytic cycle.

In the presence of intact D28 residue, YPDC exhibited both highly diminished acetolactate formation (essentially none is detected) and inhibition by the substrate (*12*). These observations suggest that the D28 residue may have dual importance, in both of which its ability to lose a proton is utilized. In the first instance [discussed in the second paper of the series (*12*)], D28 protects the post-decarboxylation intermediates from attack by pyruvate that could result in acetolactate formation. A second role for D28 would involve protection of the vacant second active site of the enzyme species with pre-decarboxylation intermediates in the first active site (depicted by ES in the Scheme 3). This would ensure an enhanced probability for the pre-decarboxylation intermediates to undergo decarboxylation (Scheme 4A), instead of substrate binding and possible LThDP formation in the second active site (Scheme 4B). Both events may reflect the same subunit conformation either when the post-decarboxylation intermediate is present in the active site or when the neighboring subunit is occupied by pre-decarboxylation intermediate(s).

It appears that H114 and/or H115 may create the site for the inhibitory pyruvate molecule for the following reason. We deduced that during the pre-decarboxylation phase of the reaction, the charge distribution at the active site is $H115^{+}$ $D28^{0}$, which is useful for attracting the first pyruvate and to form the LThDP. Once decarboxylation is completed, for the post-decarboxylation phase, the charge distribution was deduced to change to $H115^{+}$ $D28^{-}$, so as to repel the second pyruvate that could form acetolactate. With the D28 variants, the charge distribution would be the same during both phases of the reaction sequence, $H115^{+}$ $D28^{0}$, which could indeed be more attractive for a pyruvate molecule in either active site.

The Hill coefficients of both E477Q and H115F variants displayed similar pH dependencies (*11*). Given that both E477 and H115 likely form hydrogen bonds to residue D28, this similarity of Hill coefficient behavior may reflect that participation of both amino acids in the interaction between active sites is expressed through residue D28. Therefore, it is possible that the three acid−base residues (D28, H115, E477, and perhaps H114) of the active site are essential for signal transduction from one active site to another. Were this the case, then suppression of the post-decarboxylation phase of the reaction to a greater degree may help to determine the leading part of the sequence of the alternating sites mechanism. Indeed, were decarboxylation in one active site a prerequisite for the release of product from the second site, then disruption of the communication between the active sites would be expected to compromise the follow-up phase (product release) to a much greater degree than the leading phase. If the chain of the signal is broken, the decarboxylation in one active site results in sub-optimal changes at the second site, thereby leading to accumulation of post-decarboxylation intermediates. Were that the case, the equal or higher rate of acetoin formation by the variants than by wild-type YPDC may indicate that acetoin formation does not require the alternating site mechanism. Utilization of alternating sites by YPDC could be considered as an ultimate protection mechanism of YPDC from being diverted along the carboligase side-reaction pathways.

On the other hand, we also deduced (*12*) that neither D28 nor E477 was important for docking the incoming acetaldehyde which participates in acetoin synthesis. Therefore, once again, it is possible that the N4′-amino group participated to ensure correct binding of acetaldehyde and protonation of the incipient alkoxide anion. Of the four variants of E51 (E51A, E51Q, E51D, E51N) prepared in this laboratory (*39*), only the E51A variant could produce some acetoin, although with much impaired rates (0.006 unit/mg). At the same time, the E51D variant could produce acetaldehyde 50-fold less efficiently than WT PDC, with no evidence of acetoin formation. This signals that the regulation of the protonation step by the N4′-amino group is important for acetoin formation, possibly through the docking of the acetaldehyde substrate molecule, and perhaps for acetoin release as well.

An interesting, still outstanding issue concerns the step in the mechanism where hydroxide ion is released to the solution. On the basis of the above discussions, we propose that protonation of the ylide by water, once acetaldehyde is released, could be a likely candidate, since the ylide is certainly a strong base. Were this correct, ylide formation, present as a part of the cycle, might be the rate-limiting step under some conditions. The two variants E477Q and D28A and WT YPDC all gave the same rate of H/D exchange at the C2 position in nonactivated enzyme: $0.9-1.0\ s^{-1}$ at 5 °C, or approximately $10\ s^{-1}$ at room temperature (*11*). The two variants C221A and C221S are suspected to be nonactivated during the entire catalytic cycle. Their activity is equal to 10 units/mg; i.e., it is possible that ylide formation in nonactivated enzyme is the rate-limiting step. At the same time, H/D exchange in activated WT YPDC was reported to be $600\ s^{-1}$, and in activated E477Q and D28A variants, it is $30\ s^{-1}$ at 5 °C, fast enough not to be rate-limiting in any of the three cases.

## CONCLUSIONS

In addition to the scenarios analyzed, which provide the simplest explanations for the experimental observations, Scheme 3 allows for additional pathways. We believe that the wild-type YPDC follows pathway A or D in Scheme 4: we can be certain that the active sites in the functional dimer are not acting independently of one another, and the pre- and post-decarboxylation phases of the reaction are tightly coupled. Based on this coupling, the alternating sites model can explain: (a) equal rates of pre- and post-decarboxylation in WT YPDC, since two parts of the reaction are synchronized; (b) perceived participation of all active site amino acids in both pre- and post-decarboxylation steps [as suggested by the steady-state kinetics reported in the first paper (*11*), according to which both *V/K* and *V*-type kinetic terms are affected by substitutions at D28, H114, H115, and E477].

It is useful to place the findings in this paper in perspective concerning the several different regulatory mechanisms already delineated for ThDP-dependent enzymes in general, and for 2-oxo acid decarboxylases in particular.

Several enzymes (where this could be studied) were shown to possess hysteretic binding of the Mg(II) and, bonded to it by inner-sphere complexation, an oxygen from both the α- and β-phosphate of the diphosphate side chain of ThDP. This could be clearly demonstrated on the E1 component of the *E. coli* pyruvate dehydrogenase multienzyme complex (*40*).

All of the YPDCs (but not ZmPDC) are subject to substrate activation. In a series of papers from this laboratory (*18*−*22* and other references cited therein), we made a case for residue C221 being the site on YPDC where the substrate activation cascade is triggered, the information being transmitted to the active center from the substrate bound to C221 via H92 to E91 to W412 (*18*−*22, 41, 42*), to the residue adjacent to G413, the latter forming a strong hydrogen bond to the 4′-amino group of ThDP. This could be construed as an "intrasubunit" pathway. Studies in our laboratory on the E1 component of the *E. coli* pyruvate dehydrogenase multienzyme complex also pointed to a substrate activation phenomenon (*43*), whose structural origins are still unknown.

The results reported on YPDC in this and the accompanying papers (*11, 12*) have led us to conclude that there is a novel signal transduction pathway, in which there is an interaction of active sites, and in which residue D28 from one subunit and residue E477 of the second are major players in a functional dimer. We conceive of this novel signal transduction pathway as an "intersubunit" pathway, to distinguish it from the substrate activation model discussed in the previous paragraph. Our recent studies on BFD also led us to a similar proposal on the basis of pre-steady-state kinetics (*10*).

Elucidation of further structural details of this novel pathway, whether the "intrasubunit" pathway and "intersubunit" pathway are interconnected, and, of course, as to how general this "intersubunit" pathway is for ThDP enzymes, remain challenges for the future.

A mechanism related to the alternating-sites scheme here proposed appears to have also been proposed for the ThDP-dependent E1 subunit of the mammalian pyruvate dehydrogenase multienzyme complex (*45*).

## APPENDIX

*Predictions of the SHS Kinetic Model of YPDC Catalysis.* It was proposed by the groups of Schellenberger, Hübner, and Schowen (SHS) (*5, 6*) that YPDC follows the mechanism outlined in Scheme 1.

$$v = \frac{V[\mathrm{S}]^2}{A + B[\mathrm{S}] + [\mathrm{S}]^2(1 + [\mathrm{S}]/K_\mathrm{i})} \tag{A1}$$

$$V_\mathrm{max} = \frac{k_{c3}k_{c5}}{k_{c3} + k_{c5}} \tag{A2}$$

$$A = \frac{k_{a2}k_{a4}(k_{c2} + k_{c3})k_{c5}}{k_{a1}k_{a3}k_{c1}(k_{c3} + k_{c5})} \tag{A3}$$

$$B = K_\mathrm{s} = \frac{(k_{a3} + k_{a4})(k_{c2} + k_{c3})k_{c5}}{k_{a3}k_{c1}(k_{c3} + k_{c5})} \tag{A4}$$

$$K_\mathrm{a} = \frac{A}{B} = \frac{k_{a2}k_{a4}}{k_{a1}(k_{a3} + k_{a4})} \tag{A5}$$

$$\frac{K_\mathrm{a}}{K_\mathrm{s}} = \frac{k_{a2}k_{a3}k_{a4}k_{c1}(k_{c3} + k_{c5})}{k_{a1}(k_{a3} + k_{a4})^2(k_{c2} + k_{c3})k_{c5}} \tag{A6}$$

$$v = \frac{V[\mathrm{S}]^2}{K_\mathrm{a}K_\mathrm{s} + K_\mathrm{s}[\mathrm{S}] + [\mathrm{S}]^2(1 + [\mathrm{S}]/K_\mathrm{i})} \tag{A7}$$

The activity of the enzyme is described by eq A1, with the parameters of this equation derived in terms of the individual rate constants in eqs A2−A6. In terms of the particular kinetic dissociation constants $K_\mathrm{a}$ and $K_\mathrm{s}$, the general equation (A1) can be presented in the form of the Adair equation (eq A7). One of the advantages of this formalism is the separation of the purely activation pathway ($K_\mathrm{a}$) from the catalytic cycle ($K_\mathrm{s}$), which will take on special significance once we derive the corresponding Hill equation parameters.

*Derivation of the Parameters of the Hill Equation for the SHS Model.* Using the definition of the Hill equation parameters (*44*) one can derive the correlations of these parameters with the ones given by the general (or Adair) equation. According to the simple definition, the Hill coefficient ($n_\mathrm{H}$) is equal to the slope of the Hill plot at the concentration of the substrate equal to the half-saturation concentration ($S_{0.5}$):

$$n_\mathrm{H} = \frac{\mathrm{d}\{\log [v/(V_\mathrm{max} - v)]\}}{\mathrm{d}(\log [\mathrm{S}])} = \frac{[\mathrm{S}]V_\mathrm{max}\,\mathrm{d}v}{v(V_\mathrm{max} - v)\,\mathrm{d}[\mathrm{S}]} \tag{A8}$$

The half-saturation concentration, in turn, is equal to the positive solution of the rate equation with $v = V_\mathrm{max}/2$.

In terms of the SHS (eq A1), the half-saturation concentration and Hill coefficient are expressed as

$$S_{0.5} = \frac{B + \sqrt{B^2 + 4A}}{2} \tag{A9}$$

$$n_\mathrm{H} = \frac{2A + BS_{0.5}}{A + BS_{0.5}} \tag{A10}$$

In terms of the Adair-type eq A7, the resulting equations are

$$S_{0.5} = \frac{K_\mathrm{s}}{2}\left(1 + \sqrt{1 + \frac{4K_\mathrm{a}}{K_\mathrm{s}}}\right) \tag{A11}$$

$$n_\mathrm{H} = \frac{2K_\mathrm{a} + S_{0.5}}{K_\mathrm{a} + S_{0.5}} = \frac{1 + 4\alpha + \sqrt{1 + 4\alpha}}{1 + 2\alpha + \sqrt{1 + 4\alpha}} \tag{A12}$$

where $\alpha = K_\mathrm{a}/K_\mathrm{s}$. This means that if $K_\mathrm{a}/K_\mathrm{s}$ is equal to zero, the Hill coefficient is equal to 1, and if $K_\mathrm{a}/K_\mathrm{s}$ takes on increasingly larger values, the Hill coefficient asymptotically approaches 2. Therefore, both the half-saturation concentration and the Hill coefficient are monotonically increasing functions that attain values from $K_\mathrm{s}$ (B) to $+\infty$ and from 1 to 2, respectively (Figure 6). Since neither $K_\mathrm{a}$ nor $K_\mathrm{s}$ can be strictly equal to zero or infinity, those limiting values represent asymptotes for the corresponding curves.

## REFERENCES

1. Bisswanger, H., and Schellenberger, A., Eds. (1996) *Biochemistry and Physiology of Thiamin Diphosphate Enzymes*, pp 1−599, A.u.C. Intemann, Wissenschaftlicher Verlag, Prien, Germany.

2. Jordan, F., Nemeria, N., Guo, F., Baburina, I., Gao, Y., Kahyaoglu, A., Li, H., Wang, J., Yi, J., Guest, J., and Furey, W. (1998) *Biochim. Biophys. Acta 1385*, 287−306.
3. Boiteux, A., and Hess, B. (1970) *FEBS Lett. 9*, 293−296.
4. Hübner, G., Weidhase, R., and Schellenberger, A. (1978) *Eur. J. Biochem. 92*, 175−181.
5. Alvarez, F. J., Ermer, J., Hübner, G., Schellenberger, A., and Schowen, R. L. (1991) *J. Am. Chem. Soc. 113*, 8402−8409.
6. Alvarez, F., Ermer, J., Hübner, G., Schellenberger, A., and Schowen, R. (1995) *J. Am. Chem. Soc. 117*, 1678−1683.
7. Dyda, F., Furey, W., Swaminathan, S., Sax, M., Farrenkopf, B., and Jordan, F. (1993) *Biochemistry 32*, 6165−6170.
8. Arjunan, D., Umland, T., Dyda, F., Swaminathan, S., Furey, W., Sax, M., Farrenkopf, B., Gao, Y., Zhang, D., and Jordan, F. (1996) *J. Mol. Biol. 256*, 590−600.
9. Lu, G., Dobritzsch, D., König, S., and Schneider, G. (1997) *FEBS Lett. 403*, 249−253.
10. Sergienko, E. A., Wang, J., Polovnikova, L., Hasson, M. S., McLeish, M. J., Kenyon, G. L., and Jordan, F. (2000) *Biochemistry 39*, 13862−13869.
11. Liu, M., Sergienko, E. A., Guo, F., Wang, J., Tittmann, K., Hübner, G., and Jordan, F. (2001) *Biochemistry 40*, 7355−7368.
12. Sergienko, E. A., and Jordan, F. (2001) *Biochemistry 40*, 7369−7381.
13. Pastra-Landis, S. C., Evans, D. R., and Lipscomb, W. N. (1978) *J. Biol. Chem. 253*, 4624−4630.
14. LiCata, V. J., and Allewell, N. M. (1997) *Biophys. Chem. 64*, 225−234.
15. Mannervik, B. (1982) *Methods Enzymol. 87*, 370−390.
16. Segel, I. H. (1975) *Enzyme kinetics. Behavior and analysis of rapid-equilibrium and steady-state enzyme systems*, p 382, Wiley-Interscience, New York.
17. Adair, G. S. (1925) *J. Biol. Chem. 63*, 529−545.
18. Wang, J., Golbik, R., Seliger, B., Spinka, M., Tittmann, K., Hübner, G., and Jordan, F. (2000) *Biochemistry 40*, 1755−1763.
19. Wei, W., Liu, M., and Jordan, F., in preparation.
20. Baburina, I., Gao, Y., Hu, Z., Hohmann, S., Furey, W., and Jordan, F. (1994) *Biochemistry 33*, 5630−5635.
21. Baburina, I., Moore, D. J., Volkov, A., Kahyaoglu, A., Jordan, F., and Mendselsohn, R. (1996) *Biochemistry 35*, 10249−10255.
22. Baburina, I., Li, H., Furey, W., Bennion, B., and Jordan, F. (1998) *Biochemistry 37*, 1235−1244.
23. Juni, E. (1961) *J. Biol. Chem. 236*, 2302−2308.
24. Juni, E., and Heym, G. A. (1968) *Arch. Biochem. Biophys. 127*, 79−88.
25. Juni, E., and Heym, G. A. (1968) *Arch. Biochem. Biophys. 127*, 89−100.
26. Cleland, W. W. (1979) *Methods Enzymol. 63*, 500−513.
27. Kuhl, P. W. (1994) *Biochem. J. 298*, 171−180.
28. Lu, G., Dobritzsch, D., Baumann, S., Schneider, G., and König, S. (2000) *Eur. J. Biochem. 276*, 861−868.
29. Monod, J., Wyman, J., and Changeux, J. P. (1965) *J. Mol. Biol. 12*, 88−118.
30. Boyer, P. D. (1997) *Annu. Rev. Biochem. 66*, 717−749.
31. Brendza, K. M., Rose, D. J., Gilbert, S. P., and Saxton, W. M. (1999) *J. Biol. Chem. 274*, 31504−31514.
32. Sergienko, E. A., and Jordan, F. (2000) *FASEB J. 14*, A1325, Abstr. 84.
33. Jordan, F., Kuo, D. J., and Monse, E. U. (1978) *J. Am. Chem. Soc. 100*, 2872−2878.
34. Chen, L. (2000) Ph.D. Dissertation, Rutgers University Graduate Faculty at Newark, NJ, Supervised by Huskey, W. P.
35. Stivers, J. T., and Washabaugh, M. W. (1993) *Biochemistry 32*, 13472−13482.
36. Jordan, F., Li, H., and Brown, A. (1999) *Biochemistry 38*, 6369−6373.
37. Liu, M., Zhong, Z., and Jordan, F., in preparation.
38. Guo, F., Zhang, D., Kahyaoglou, A., Farid, R. S., and Jordan, F. (1998) *Biochemistry 37*, 13379−13391.
39. Gao, Y. (2000) Ph.D. Dissertation, Rutgers University Graduate Faculty at Newark, NJ.
40. Yi, J., Nemeria, N., McNally, A., Jordan, F., Guest, J. R., and Machado, R. (1996) *J. Biol. Chem. 271*, 33192−33200.
41. Li, H., and Jordan, F. (1999) *Biochemistry 38*, 10004−10012.
42. Li, H., Furey, W., and Jordan, F. (1999) *Biochemistry 38*, 9992−10003.
43. Nemeria, N., Volkov, A., Brown, A., Yi, J., Zipper, L., Guest, J. R., and Jordan, F. (1998) *Biochemistry 37*, 911−922.
44. Dahlquist, F. W. (1978) *Methods Enzymol. 48*, 270−299.
45. Khailova, L. S., Korochkina, L. G., and Severin, S. E. (1989) *Ann. N.Y. Acad. Sci. 573*, 37−54.

BI002857E